AD_____

Award Number: W81XWH-11-1-0819

TITLE: An Implantable Neuroprosthetic Device to Normalize Bladder Function after SCI

PRINCIPAL INVESTIGATOR: Changfeng Tai, PhD

CONTRACTING ORGANIZATION: University of Pittsburgh

REPORT DATE: October 2012

TYPE OF REPORT: Annual report

PREPARED FOR: U.S. Army Medical Research and Materiel Command
Fort Detrick, Maryland 21702-5012

DISTRIBUTION STATEMENT: Approved for Public Release;
Distribution Unlimited

The views, opinions and/or findings contained in this report are those of the author(s) and should not be construed as an official Department of the Army position, policy or decision unless so designated by other documentation.

REPORT DOCUMENTATION PAGE

Form Approved
OMB No. 0704-0188

1. REPORT DATE	2. REPORT TYPE	3. DATES COVERED
October 2012	Annual report	22 September 2011-21 September 2012

4. TITLE AND SUBTITLE
An Implantable Neuroprosthetic Device to Normalize Bladder Function after SCI

5a. CONTRACT NUMBER

5b. GRANT NUMBER
W81XWH-11-1-0819

5c. PROGRAM ELEMENT NUMBER

6. AUTHOR(S)
Changfeng Tai, PhD

E-Mail: cftai@pitt.edu

5d. PROJECT NUMBER

5e. TASK NUMBER

5f. WORK UNIT NUMBER

7. PERFORMING ORGANIZATION NAME(S) AND ADDRESS(ES)
University of Pittsburgh
Pittsburgh, PA 15213-3320

8. PERFORMING ORGANIZATION REPORT NUMBER

9. SPONSORING / MONITORING AGENCY NAME(S) AND ADDRESS(ES)
U.S. Army Medical Research and Materiel Command
Fort Detrick, Maryland 21702-5012

10. SPONSOR/MONITOR'S ACRONYM(S)

11. SPONSOR/MONITOR'S REPORT NUMBER(S)

12. DISTRIBUTION / AVAILABILITY STATEMENT
Approved for Public Release; Distribution Unlimited

13. SUPPLEMENTARY NOTES

14. ABSTRACT

The long-term goal of our project is to develop a novel neuroprosthetic device to restore the functions of the urinary bladder for SCI people without further damaging the nervous system. Advanced technologies in electrical and computer engineering will be applied to design the novel neuroprosthetic device. Based on our previous studies, we propose in this project to use pudendal nerve stimulation and blockade to restore both continence and micturition after SCI. Our strategy does not require sacral posterior root rhizotomy, preserves the spinal reflex functions of the bowel and sexual organs, and more importantly provides the opportunity for SCI people to benefit from any advance in neural regeneration and repair techniques in the future. During the last year, we have developed the first implantable stimulator and successfully tested it in both anesthetized animals and awake chronic spinal cord injured animals. Efficient voiding was induced by the implanted stimulator in awake chronic spinal cord injured animals. These results indicated that an implantable stimulator for pudendal nerve stimulation/blockade could be developed for human subjects to restore both continence and micturition functions after SCI.

15. SUBJECT TERMS
Spinal cord injury, micturition, bladder, stimulator, block

16. SECURITY CLASSIFICATION OF:			17. LIMITATION OF ABSTRACT	18. NUMBER OF PAGES	19a. NAME OF RESPONSIBLE PERSON
					USAMRMC
a. REPORT	b. ABSTRACT	c. THIS PAGE			19b. TELEPHONE NUMBER *(include area code)*
U	U	U	UU	79	

Table of Contents

Introduction

The long-term goal of our project is to develop a novel neuroprosthetic device to restore the functions of the urinary bladder for SCI people without further damaging the nervous system. Advanced technologies in electrical and computer engineering will be applied to design the novel neuroprosthetic device. Based on our previous studies [1-4], we propose in this project to use pudendal nerve stimulation and blockade to restore both continence and micturition after SCI. Our strategy does not require sacral posterior root rhizotomy, preserves the spinal reflex functions of the bowel and sexual organs, and more importantly provides the opportunity for SCI people to benefit from any advance in neural regeneration and repair techniques in the future. During the last year, we have developed the first implantable stimulator and successfully tested it in both anesthetized animals and awake chronic spinal cord injured animals. Efficient voiding was induced by the implanted stimulator in awake chronic spinal cord injured animals. These results indicated that an implantable stimulator for pudendal nerve stimulation/blockade could be developed for human subjects to restore both continence and micturition functions after SCI.

Body

During the last year, we have made significant progress on both specific aims proposed in our original grant applications. The specific aims of this project are: Aim #1: Design and develop an implantable stimulator to activate and/or block the pudendal nerves. Aim #2: Test the implantable stimulator in awake chronic SCI animals.

Specific Aim #1

The proposed neuroprothetic system as shown in Fig.1 includes an implanted stimulator, an external control device, and an external charging device. During the last funding year, we have successfully developed the first prototype of the proposed system including a small (4x 5.5 x 1.4 cm) implantable stimulator that can be wirelessly controlled by an external USB controller (see Fig.2). This small implantable stimulator can also be charged externally through a wireless

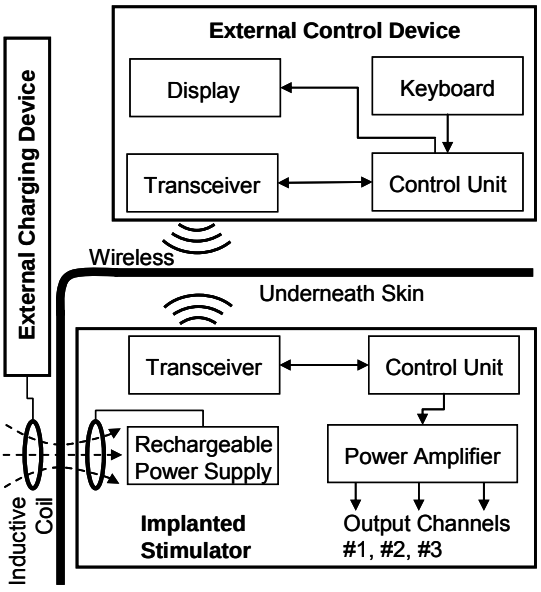

Figure 1: The proposed neuroprosthetic device.

Figure 2: The implantable stimulator and USB controller.

charging device (not shown in Fig.2). We also developed the software for computer to send control signal via the USB controller to wirelessly control the output of the implantable stimulator.

The implantable stimulator has 3 output channels. One channel provides the low frequency output (1-100 Hz, 0-11 V) for bladder inhibition or excitation [2][4]. The other channels provide the high frequency output (5k-20k Hz, 0-11 V) for pudendal nerve block [1][3]. We have successfully tested this implantable stimulator in 6 anesthetized cats. Efficient voiding (>80%, Fig.3) was induced in the 6 cats by wireless control through the USB controller using a computer. Fig.3 (left) shows that 10 kHz pudendal nerve block combined with 20 Hz pudendal nerve stimulation induced efficient voiding (88%) in an anesthetized cat, while Fig.3 (right) shows the summarized results from the 6 cats.

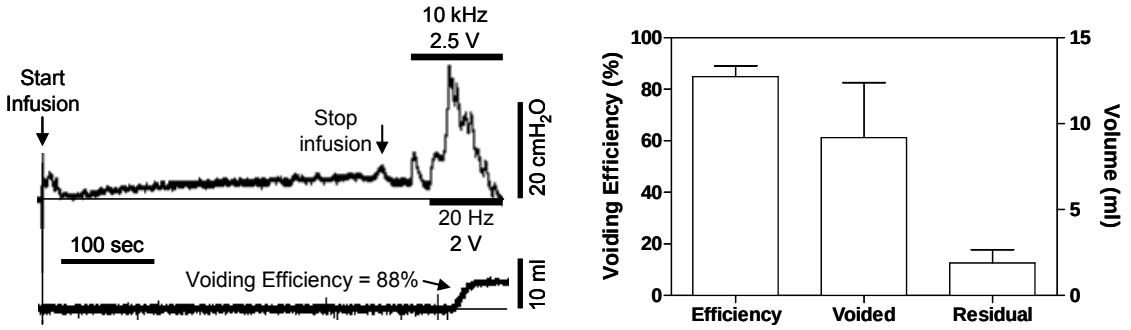

Figure 3: Efficient voiding induced in anesthetized cats by the implantable stimulator.

Specific Aim #2

We also successfully implanted this stimulator underneath the skin on the low back of an awake cat after 2 month SCI and chronically tested the stimulator to induce voiding in a 2-week period. In this first implantation, only one cuff electrode was implanted on the left pudendal nerve. Therefore, voiding induced by intermittent stimulation was tested but pudendal nerve block during voiding was not tested. The output of the implantable stimulator was successfully controlled by the USB controller through a portable computer in 1-2 meter distance. The external charging device fully re-charged the implanted stimulator in about 15-20 minutes.

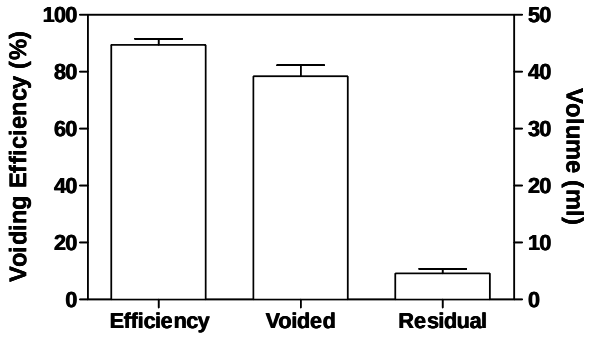

Figure 4: Voiding efficiency in an awake cat after 2 month SCI

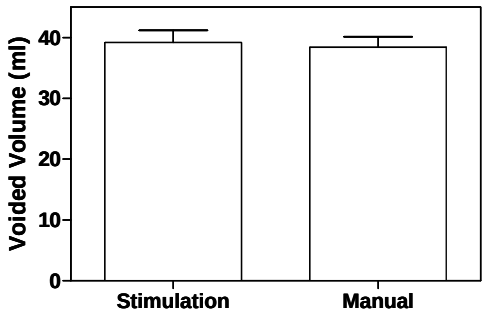

Figure 5: Voided volume in an awake cat after 2 month SCI

During the experiment under awake condition, the cat was lying quietly on a table. Intermittent stimulation of 10-20 seconds on and 20-30 seconds off (5-6 V, 40 Hz, 0.2 ms) induced efficient (about 90%) voiding of about 40 ml with a small residual volume (3-5 ml)

during the 2-week test period (Fig.4). The voided volume induced by stimulation was almost same as the voided volume induced by manual expression during the 10 day period before the stimulation experiments (Fig.5).

Finally, during acute experiments under anesthesia the bladder pressure was measured during the stimulation-induced voiding (Fig.6) Intermittent stimulation of 10-20 second on and off at 3-4 V induced bladder pressure less than 40 cmH_2O and failed to induce voiding. Voiding was only induced at 5-6 V when large (>40 cmH_2O) amplitude bladder contraction was induced. Voiding occurred intermittently only at the time when the short burst stimulation was off (i.e. post-stimulus voiding).

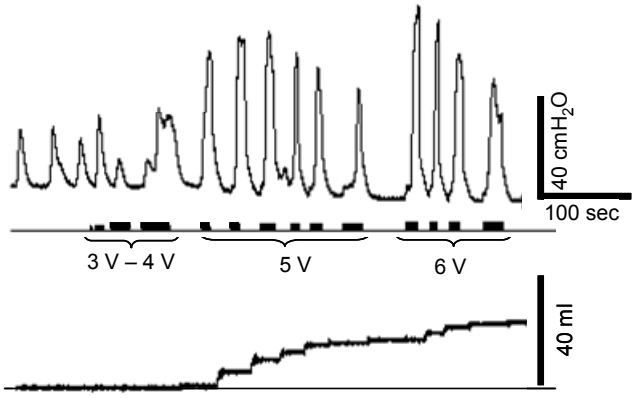

Figure 6: Voiding pressure induced by intermittent stimulation.

Key Research Accomplishments

- Developed the first prototype of a wireless controlled, wireless chargeable, small implantable stimulator
- Successfully implanted the stimulator in a chronic SCI cat and tested in a 2-week period
- Successfully induced efficient voiding in an awake cat after 2 month chronic SCI

Reportable Outcomes

Manuscript

[1] Shouguo Zhao, Jicheng Wang, James R. Roppolo, William, C. de Groat, Changfeng Tai, "Mechanisms underlying non-monotonic block of conduction in unmyelinated axons by high-frequency biphasic stimulation", Journal of Neural Engineering, 2012. submitted

[2] Shouguo Zhao, Jicheng Wang, James R. Roppolo, William, C. de Groat, Changfeng Tai, "Non-monotonic block of conduction in myelinated axons by high-frequency biphasic electrical stimulation", Journal of Computational Neuroscience, 2012. submitted

Abstract

[1] Changfeng Tai, "An implantable neuroprosthetic device to restore bladder function after SCI". Military Health System Research Symposium, Fort Lauderdale, Florida, 2012

[2] Jicheng Wang, Shouguo Zhao, James R. Roppolo, William C. de Groat, Changfeng Tai, "Mechanisms underlying non-monotonic block of unmyelinated axons by high-frequency biphasic stimulation". 42nd Annual Meeting of Society for Neuroscience, New Orleans, 2012.

Conclusion

Our progress in the first year has produce the first implantable stimulator enabling us in the next 2 years to further investigate novel nerve stimulation/block strategies to restore bladder functions in awake cats after chronic SCI. The success of our project will create a novel implantable neuroprosthesis to restore both continence and micturition functions for SCI people. It will fundamentally change the current medical treatments for the lower urinary tract dysfunctions after SCI. Daily urethral catheterization will not be the norm for SCI. Frequent infection of the lower urinary tract will be eliminated. The quality of life will be improved greatly for both SCI people and their family.

References

[1] Changfeng Tai, James R. Roppolo and William C. de Groat , "Block of external urethral sphincter contraction by high frequency electrical stimulation of pudendal nerve", Journal of Urology, Vol.172, PP2069-2072, 2004.

[2] Changfeng Tai, Stanley E. Smerin, William C. de Groat and James R. Roppolo, "Pudendal-to-bladder reflex in chronic spinal cord injured cat", Experimental Neurology, Vol.197, PP225-234, 2006.

[3] Changfeng Tai, Jicheng Wang, Xianchun Wang, James R. Roppolo and William C. de Groat, "Voiding reflex in chronic spinal cord injured cats induced by stimulating and blocking pudendal nerves", Neurourology and Urodynamics, Vol.26, PP879-886, 2007.

[4] Changfeng Tai, Jicheng Wang, Xianchun Wang, William C. de Groat, and James R. Roppolo, "Bladder inhibition and voiding induced by pudendal nerve stimulation in chronic spinal cord injured cats", Neurourology and Urodynamics, Vol. 26, PP570-577, 2007.

Appendices

[1] Shouguo Zhao, Jicheng Wang, James R. Roppolo, William, C. de Groat, Changfeng Tai, "Mechanisms underlying non-monotonic block of conduction in unmyelinated axons by high-frequency biphasic stimulation", Journal of Neural Engineering, 2012. submitted

[2] Shouguo Zhao, Jicheng Wang, James R. Roppolo, William, C. de Groat, Changfeng Tai, "Non-monotonic block of conduction in myelinated axons by high-frequency biphasic electrical stimulation", Journal of Computational Neuroscience, 2012. submitted

[3] Changfeng Tai, "An implantable neuroprosthetic device to restore bladder function after SCI". Military Health System Research Symposium, Fort Lauderdale, Florida, 2012

[4] Jicheng Wang, Shouguo Zhao, James R. Roppolo, William C. de Groat, Changfeng Tai, "Mechanisms underlying non-monotonic block of unmyelinated axons by high-frequency biphasic stimulation". 42th Annual Meeting of Society for Neuroscience, New Orleans, 2012.

Mechanisms Underlying Non-monotonic Block of Conduction in Unmyelinated Axons by High-Frequency Biphasic Stimulation

Shouguo Zhao [1,2], Jicheng Wang [1], James R. Roppolo [3],
William C. de Groat [3], Changfeng Tai [1]

[1] Department of Urology, University of Pittsburgh, Pittsburgh, PA
[2] Department of Biomedical Engineering, Beijing Jiaotong University, P.R. China
[3] Department of Pharmacology and Chemical Biology, University of Pittsburgh, PA

Correspondence to:

Changfeng Tai, Ph.D.
Department of Urology
University of Pittsburgh
700 Kaufmann Building
Pittsburgh, PA15213, USA
Phone: 412-692-4142
Fax: 412-692-4380
Email: cftai@pitt.edu

Abstract - Axonal conduction block induced by high-frequency biphasic electrical current is investigated using a lumped circuit model of the unmyelinated axon based on Hodgkin-Huxley equations. Axons of different diameters (1 and 2 μm) can be blocked completely when the stimulation frequency is between 5 kHz and 100 kHz. The non-monotonic relationship between block threshold and stimulation frequency, recently discovered in unmyelinated axons of sea-slugs and frogs, is successfully reproduced. Our simulation reveals that complete deactivation of sodium channels by the high-frequency (> 20 kHz) stimulation is the mechanism underlying the conduction block. The decrease in block threshold as the frequency increases above 20 kHz is mainly determined by the passive axonal membrane properties. At a relatively higher frequency (>30 kHz), the high-frequency blocking stimulation can quickly deactivate the sodium channels at the beginning of the stimulation, thereby avoiding the generation of initial action potentials. This simulation study further increases our understanding of conduction block in unmyelinated axons induced by high-frequency biphasic electrical current, and can guide future animal experiments as well as optimize stimulation parameters that might be used for electrically induced nerve block in clinical applications.

Key Words: nerve, block, simulation, high-frequency, model.

I. INTRODUCTION

Blocking nerve conduction by high-frequency (kHz) biphasic electrical current has recently been investigated extensively due to its potential clinical applications to treat obesity [1]-[2], restore lower urinary tract function after spinal cord injury [3], or suppress chronic pain originating from a site of peripheral nerve injury [4]. However, the mechanisms underlying this nerve block are still unclear [5][6]. Understanding the mechanisms of nerve conduction block induced by high-frequency biphasic electrical current will be very useful in developing new nerve blocking methods, optimizing stimulation parameters, or improving the efficacy of blocking nerves in different clinical applications.

Currently there are two hypotheses regarding the possible mechanisms underlying axonal conduction block using frequencies ranging between 5 kHz and 10 kHz. One hypothesis [6]-[8] proposes that high-frequency biphasic electrical current induces both depolarization and hyperpolarization of the axon membrane under the block electrode. The alternating depolarization and hyperpolarization is so fast that the potassium channels, which have slower kinetics than sodium channels, are constantly open at a minimal stimulation frequency of about 5 kHz. Therefore when the axon membrane under the block electrode is depolarized by the high-frequency stimulation, large potassium current flows outward at the same time when sodium current flows inward. Because action potential generation requires an inward sodium current followed by a delayed outward potassium current, the constantly opened potassium channels eliminate

the delay between sodium and potassium currents, thereby causing a failure in initiating an action potential at the block electrode by either high-frequency stimulation or an in-coming action potential (i.e. conduction block). A second hypothesis proposes that high-frequency biphasic electrical current induces a constant depolarization of the axon membrane under the block electrode, which causes sodium channel inactivation and thereby conduction block [5][9].

Due to the difficulties in recording the ion channel activity in axonal nodes during high-frequency biphasic electrical stimulation, the two hypotheses have been mainly tested by modeling and computer simulation [5]-[9]. These simulation studies have been successful in reproducing many phenomena observed in animal experiments, for example the block threshold intensity monotonically increases as the stimulation frequency increases [7]-[11]. However, recent animal studies [12][13] discovered that this monotonic relationship does not hold in unmyelinated axons where the block threshold intensity only increases with frequency up to about 12-15 kHz and then decreases as the stimulation frequency further increases. This discovery provides a new challenge and/or opportunity for testing the different hypotheses regarding the blocking mechanisms.

Base on the hypothesis that high-frequency biphasic electrical current at a minimal stimulation frequency about 5 kHz induces a constant opening of potassium channels [6]-[8], it is logical to think that a further increase in stimulation frequency to 12-15 kHz might drive the sodium channel to a steady state (i.e. constantly activated, deactivated, or inactivated). Therefore, it is possible that the decrease in block threshold at a stimulation

frequency above 12-15 kHz as observed in recent animal studies of unmyelinated axons could be caused by a change in sodium channel state induced by the high-frequency biphasic electrical current. Therefore, in this study we employed an unmyelinated axonal model (Hodgkin-Huxley model) to simulate the conduction block and determine: 1. if the model can reproduce the decrease in block threshold at frequencies above 12-15 kHz; 2. what happens to the sodium and potassium channels when the block threshold starts to decrease with increasing frequency. Answering these questions will not only test the hypotheses and reveal the biophysics underlying the nerve conduction block, but may also facilitate clinical applications of nerve conduction block induced by high-frequency biphasic electrical current [1]-[4].

II. METHODS

The unmyelinated axon model (Fig.1) consists of a 9-mm-long axon segmented into many small cylinders of length $\triangle x$ = 0.25 mm, each of which is modeled by a resistance-capacity circuitry. The ionic currents passing through the variable membrane resistance are described by Hodgkin–Huxley equations [14]. Two monopolar electrodes (with the indifferent electrodes at infinity) are placed at 1 mm distance from the unmyelinated axon. One is the block electrode at the 6 mm location along the axon, where the high-frequency biphasic electrical current is delivered. The other is the test electrode at the 3 mm location, which delivers an uniphasic single pulse (pulse width: 0.1 ms; intensity: 10-15 mA) to evoke an action potential that can propagate through the site

of the block electrode. The test electrode is always the cathode (negative pulse). The block electrode always delivers the high-frequency biphasic current with the cathodal phase first.

We assume that the unmyelinated axon is in an infinite homogeneous medium (resistivity $\rho_e = 300\ \Omega$cm). After neglecting the small influence of the axon in the homogeneous medium, the extracellular potential $V_{e,n}$ at the nth segment along the axon can be described by:

$$V_{e,n} = \frac{\rho_e}{4\pi}\left[\frac{I_{block}(t)}{\sqrt{(n\Delta x - x_0)^2 + z_0^2}} + \frac{I_{test}(t)}{\sqrt{(n\Delta x - x_1)^2 + z_1^2}}\right]$$

Where $I_{block}(t)$ is the high-frequency biphasic current delivered to the block electrode (at location x_0 = 6 mm, z_0 = 1 mm); $I_{test}(t)$ is the single test pulse delivered to the test electrode (at location x_1 = 3 mm, z_1 = 1 mm).

The change of the membrane potential V_n at the nth segment of the unmyelinated axon is described by:

$$\frac{dV_n}{dt} = \left[\frac{d}{4\rho_i}\left(\frac{V_{n-1} - 2V_n + V_{n+1}}{\Delta x^2} + \frac{V_{e,n-1} - 2V_{e,n} + V_{e,n+1}}{\Delta x^2}\right) - I_{i,n}\right] / c_m$$

Where V_n=$V_{a,n}$-$V_{e,n}$-V_{rest}; $V_{a,n}$ is the intracellular potential at the nth segment; $V_{e,n}$ is the extracellular potential at the nth segment; V_{rest} is the resting membrane potential; d is the unmyelinated axon diameter; ρ_i is the resistivity of axoplasm (34.5 Ωcm); c_m is the capacity of the membrane (1 uF/cm^2); $I_{i,n}$ is the ionic current at the nth segment described by Hodgkin–Huxley equations (see appendix) [14]-[16].

The model equations were solved by Runge-Kutta method [17] with a time step of

0.2 μsec at room temperature (T = 18.5 °C). The simulation was always started at initial condition $V_n = 0$. The membrane potentials at the two end segments of the modeled axon were always equal to the membrane potentials of their closest neighbors, which implemented sealed boundary conditions (no longitudinal currents) at the two ends of the modeled axon. The block threshold intensity was determined with a resolution of 1 mA.

III. RESULTS

A. Non-monotonic blocking response to high-frequency biphasic electrical stimulation

Fig.2 shows that the Hodgkin–Huxley model can successfully simulate the conduction block in unmyelinated axons induced by high-frequency (80 kHz) biphasic electrical current in a small unmyelinated axon of 1 μm diameter. In Fig.2 (a) the 80 kHz blocking stimulation (45 mA) gradually hyperpolarizes [also see Fig.4 (a)] the axon membrane at the block electrode without generating initial action potentials. At 5 ms after the start of blocking stimulation, the test electrode delivers a single pulse that generates another action potential propagating toward the block electrode [see the white arrow in Fig.2 (a)]. This action potential fails to propagate through the block electrode due to the presence of the high-frequency biphasic electrical current. However, at a lower stimulation intensity [44 mA in Fig.2 (b)] the 80 kHz stimulation does not block nerve conduction and the action potential propagates through the site of block electrode.

Fig.3 shows the intensity threshold for inducing conduction block at different frequencies (5-100 kHz) for small unmyelinated axons of diameters between 1 μm and 2

μm. The block threshold increases initially and then decreases with increasing stimulation frequency, showing a non-monotonic relationship between block threshold and stimulation frequency. The block threshold peaks between 13 kHz and 16 kHz, which agrees very well with recent animal studies [12][13] indicating that the block threshold peaks at a frequency of 12-15 kHz.

B. Mechanism underlying the non-monotonic relationship between block threshold and stimulation frequency

Our previous simulation studies [7][18] revealed that the monotonic increase in block threshold at frequencies below 10 kHz is due to a constant activation of potassium channels by the high-frequency biphasic current. In order to understand why the block threshold starts to decrease at frequencies above 20 kHz, we further investigated the changes in membrane potential, ionic currents, and activation/inactivation of the sodium and potassium channels along a 1-μm-diameter axon at different locations near the block electrode. Fig.4 shows the same simulation as in Fig.2 (a) including more detailed information for the 5 consecutive axon segments at distances of 0-1 mm from the block electrode (the location at 0 mm is under the block electrode) during blocking stimulation at 80 kHz.

At locations approaching the block electrode, the amplitude of action potential gradually declined [Fig.4 (a)]. Action potential propagation is completely abolished at the location (0 mm) under the block electrode, where the axon membrane is hyperpolarized

to about -100 mV [(-30 mV) + (-70 mV resting potential), see Fig.4 (a)] and no sodium or potassium currents are generated by the in-coming action potential [Fig.4 (b) and (c)]. The behavior of the action potential and ionic currents can be explained by the activation/inactivation of the sodium and potassium channels as shown in Fig.4 (d)-(f). As the action potential propagates toward the block electrode, the activation (m) of sodium channels progressively declines at the locations close to the block electrode (0-0.5 mm) and eventually becomes almost zero (i.e. completely deactivated) at the location (0 mm) under the block electrode [Fig.4 (d)]. Meanwhile, inactivation (h) of sodium channels is minimal (≈ 1) at the location (0 mm) under the block electrode [Fig.4 (e)]. The combination of activation (m) and inactivation (h) of sodium channels [Fig.4 (d) and (e)] determines that the amplitude of sodium current gradually attenuates at the locations close to the block electrode and eventually disappears at the location (0 mm) under the block electrode [Fig.4 (b)]. Therefore the conduction block is due to a complete deactivation of the sodium channels under the block electrode [Fig.4 (d)]. The same blocking mechanism is observed for different diameter axons (1 and 2 μm) at the frequencies greater than 13 kHz and 16 kHz respectively (Fig.3).

Meanwhile, the changes in potassium activation (n) induced by the action potentials also gradually disappear at the locations close to the block electrode [Fig.4 (f)] because the potassium channels are also gradually deactivated. The level of potassium channel activation is minimal at the location (0 mm) under the block electrode, which results in no potassium current at this location [Fig4 (c)]. Therefore, 80 kHz stimulation completely

deactivates both sodium and potassium channels at the location under the block electrode.

At the blocking threshold intensity, the effect of different stimulation frequencies on activation and inactivation of sodium and potassium channels at the location under the block electrode is shown in Fig.5. At the frequency range of 5-10 kHz the sodium channel activation (m) is still oscillatory during the blocking stimulation [Fig.5 (a)] while the inactivation (h) is at a level around 0.3-0.6 [Fig.5 (b)]. This allows the sodium channels to open and generate large pulsed inward sodium currents during blocking stimulation as has been revealed in our previous studies [7][18]. Meanwhile, at 5-10 kHz the potassium channel is constantly open with its activation (n) around 0.5 [Fig.5 (c)]. Our previous studies [7][18] show that the constantly opened potassium channels generate large outward potassium currents negating the inward sodium currents and causing conduction block. As the frequency increases from 5 kHz to 10 kHz, a higher stimulation intensity is required in order to maintain the potassium channel open at the level $n \approx 0.5$ [Fig.5 (c)] [7][18], thereby resulting in a monotonic increase in block threshold.

However, as the stimulation frequency increases above 20 kHz the sodium activation (m) becomes almost zero [i.e., completely deactivated, Fig.5 (a)] while the inactivation (h) is close to one [i.e., minimal inactivation, Fig.5 (b)]. The complete deactivation of sodium channel during high-frequency stimulation results in axonal conduction block. In addition, potassium channels are also completely deactivated as the frequency increases above 20 kHz [Fig.5 (c)]. Complete deactivation of sodium channels requires a lower stimulation intensity as the frequency increases above 20 kHz [Fig.5 (a)], thereby resulting in a

monotonic decrease in block threshold.

At frequencies above 20 kHz, the high-frequency stimulation must drive the sodium channel to a certain level of deactivation in order to achieve the conduction block (Fig. 6). At a specific frequency (80 kHz), a stimulation of higher intensity deactivates the sodium channel more than the stimulation of a lower intensity [Fig.6 (a)]. This explains why a minimal stimulation intensity (i.e. block threshold) is required at a specific frequency to block the nerve conduction (Fig.3). Meanwhile, at a specific stimulation intensity (45 mA), stimulation at a higher frequency deactivates the sodium channel more than stimulation at a lower frequency [Fig.6 (d)]. Therefore, in order to deactivate the sodium channels to a level ($m \approx 0$) for inducing a conduction block, the stimulation at a higher frequency requires a lower intensity (Fig.3). At the block threshold (45 mA at 80 kHz) the sodium channels are completely deactivated within 2 ms from the beginning of the stimulation [Fig.6 (a)/(d)], while the sodium channel inactivation [Fig.6 (b)/(e)] and the potassium channel activation [Fig.6 (c)/(f)] are only changed slightly during this time period.

C. Response of an axon with passive membrane properties to high-frequency biphasic electrical stimulation

Since our results indicate that both sodium and potassium channels are completely deactivated by high-frequency (> 20 kHz) stimulation to induce nerve block, the axonal membrane becomes a passive membrane under the block electrode. Therefore, it is

logical to hypothesize that the relationship between stimulation frequency and block threshold at frequencies greater than 20 kHz (see Fig.3) is mainly determined by the passive properties of the axonal membrane. To test this hypothesis we removed both sodium and potassium channels in the Hodgkin-Huxley model but retained the normal leakage ion channels, i.e. the ionic current at the n^{th} segment of the axon is now described by $I_{i,n} = g_L(V_n - V_L)$ (see Appendix for comparison). The responses of this passive axonal model to high-frequency stimulation are presented in Fig.7.

When the high-frequency (80 kHz) stimulation of block threshold intensity (45 mA) is applied to the passive axon, it hyperpolarizes the axonal membrane under the block electrode (Fig.7 A) and the hyperpolarization oscillates around -98 mV [(-28 mV) + (-70 mV resting potential), see the solid line in Fig.7 B]. A similar response is also induced in the active axon (Hodgkin-Huxley model) with a slightly greater hyperpolarization oscillating around -100 mV [(-30 mV) + (-70 mV resting potential), see the dashed line in Fig.7 B]. This result confirms that the hyperpolarization induced by high-frequency stimulation under the block electrode is mainly due to the passive properties of the axon that becomes a distributed passive resistance-capacitance cable model (see Fig.1).

When stimulations of different frequencies (40-100 kHz) are applied at their block threshold intensities to the passive axon, they produce a hyperpolarization under the block electrode oscillating around the same potential -98 mV [(-28 mV) + (-70 mV resting potential), see Fig.7 C]. However, a higher frequency requires a lower intensity in order to hyperpolarize the passive membrane to the same membrane potential (see the

legends in Fig.7 C). This explains why the block threshold in Fig.3 decreases with increasing frequencies greater than 20 kHz.

In summary, the results from passive axon further confirm the hypothesis that the high-frequency (> 20 kHz) stimulation completely closes both sodium and potassium channels under the block electrode (Figs.4-6) causing the axon membrane under the block electrode to be a passive membrane. Therefore, the relationship between stimulation frequency and block threshold at frequencies greater than 20 kHz (see Fig.3) is mainly determined by the passive properties of the axonal membrane (Fig.7 C).

D. Initial action potential generation by high-frequency biphasic electrical current

At the block thresholds and frequencies below 10 kHz, the high-frequency biphasic current always generates initial action potentials before it blocks nerve conduction [6][16]. These initial action potentials are also observed at 20 kHz [Fig.8 (a)], but not at 40 kHz [Fig.8 (b)]. This is because at the block thresholds and frequencies above 30 kHz the sodium channels at the location under the block electrode are quickly deactivated [$m \approx 0$, Fig.9 (a)] once the blocking stimulation starts. This quick and complete deactivation of sodium channels eliminates the initiation of any action potentials although sodium inactivation [Fig.9 (b)] and potassium activation [Fig.9 (c)] are only changed slightly at the beginning of high-frequency (>30 kHz) stimulation. This result further confirms that the complete deactivation of sodium channels is the cause of nerve conduction block because it also blocks the generation of action potential that is supposed to be induced by

the high-frequency stimulation at the initiation of the stimulation.

IV. DISCUSSION

This study employed the Hodgkin–Huxley axonal model to simulate nerve conduction block in unmyelinated axons during high-frequency (up to 100 kHz) biphasic electrical stimulation (Fig.2) and reproduced the non-monotonic relationship between block threshold and stimulation frequency (Fig.3), which was recently discovered in unmyelinated axons of sea-slugs [12] and frogs [13]. In addition, our study revealed that deactivation of sodium channels by the high-frequency stimulation is the mechanism underlying the decrease in block threshold at frequencies above 20 kHz (Figs.4-7). This nerve blocking mechanism has the potential to eliminate the action potentials elicited at the beginning of blocking stimulation at relatively higher frequencies (>30 kHz) (Figs.8-9).

This study and our previous studies [7][18] using an unmyelinated axonal model (Hodgkin–Huxley model) have successfully predicted not only the minimal blocking frequency (5 kHz) [12][13][19]-[21] but also the frequencies (13-16 kHz) where the block threshold starts decreasing [12][13]. These results indicate that the kinetics of ion channel gating plays a major role in the conduction block induced by high-frequency biphasic electrical current. For example, the kinetics of the potassium channel are slow compared to the sodium channel, and therefore this channel does not follow high-frequencies of stimulation. Thus the potassium channel becomes constantly open as

the frequency increases to the minimal blocking frequency of about 5 kHz. This potassium channel mechanism governs the monotonic increase in block threshold as the stimulation frequency is increased up to 10 kHz (Fig.3). As the frequency increases further, it saturates the faster kinetics of the sodium channel at about 13-16 kHz (Fig.3) causing the sodium channel to lose its ability to follow the high-frequency stimulation and becomes completely deactivated [Fig.4 (d) and Fig.5 (a)]. This sodium channel mechanism is responsible for the conduction block [Figs.4-6 and Fig.9]. The monotonic decrease of block threshold for frequencies above 20 kHz (Fig.3) is mainly determined by the passive axonal membrane properties (Fig.7) since the high-frequency stimulation completely closes both sodium and potassium channels. Therefore, the non-monotonic relationship between the block threshold and stimulation frequency, which was discovered recently in unmyelinated axons of sea-slugs [12] and frogs [13] and reproduced in this stimulation study, can be fully explained by the kinetics of potassium and sodium channels during high-frequency biphasic electrical stimulation.

This study challenges the hypothesis that the high-frequency biphasic current induces a depolarization under the block electrode causing sodium channel inactivation and thereby conduction block [5][9]. It is difficult to explain how depolarization-induced sodium channel inactivation can produce the observed [12][13] non-monotonic blocking response to high-frequency biphasic electrical stimulation? What might be changed during depolarization-induced block that could account for the decreasing block threshold as the frequencies are increased above 20 kHz?

Our results show that high-frequency blocking stimulation actually induces a hyperpolarization rather than a depolarization under the block electrode [Fig.2, Fig.4 (a), and Fig.7] leading to sodium channel deactivation rather than sodium channel inactivation that is minimal [$n \approx 1$, see Fig.4 (e) and Fig.5 (b)] at frequencies above 20 kHz.

Based on our hypothesis about the role of different ion channel kinetics in conduction block, it would be logical to predict that a non-monotonic relationship between the block threshold and the stimulation frequency should also exist in myelinated axons. However, currently the results obtain from animal studies [10][11][13] only show that the block threshold monotonically increases as the frequency increases up to 50 kHz. Since the sodium channel in myelinated axons [22] has a much faster kinetics than in unmyelinated axons [14], it is possible that a frequency greater than 50 kHz might be needed in order to drive the sodium channels in myelinated axons to a completely deactivated state. Our recent simulation study [23] using a myelinated axon model (Frankenhaeuser-Huxley model) did not observe a decrease in block threshold at frequencies up to 100 kHz for axons of diameter 10-20 μm, suggesting that frequencies greater than 100 kHz might be required to observe a decrease in block threshold in large myelinated axons. Clearly, more studies are warranted to investigate nerve conduction block at frequencies above 50 kHz for myelinated axons.

Understanding the different blocking mechanisms might help to optimize the blocking stimulation waveforms for different clinical applications. One of the clinical

requirements in applying the high-frequency nerve block to suppress chronic pain of peripheral origin is to minimize the initial nerve firing induced by the blocking stimulation. Both cooling and DC current have been investigated in an attempt to block the initial firing caused by the high-frequency stimulation [24][25]. However these blocking methods could cause significant nerve damage in clinical applications. A recent study [26] also showed that the initial firing can be significantly reduced by first applying a 30 kHz stimulation and then shifting the stimulation to a lower frequency (10 kHz). Our current study indicates that in small unmyelinated axons (i.e., the nociceptive C-fibers) the initial nerve firing can be eliminated at the stimulation frequency above 30 kHz (Figs. 8-9) since the sodium channels can be quickly deactivated within 2 ms from the beginning of the stimulation [Fig.6 (a)/(d) and Fig.9 (a)]. Meanwhile the stimulation intensity required to block these axons at the higher frequencies (>30 kHz) may not necessarily be greater than the intensity at frequencies below 10 kHz due to the non-monotonic intensity-frequency relationship (Fig.3) [12][13]. These results suggest that a higher stimulation frequency (30-100 kHz) might be more preferable in clinical applications aimed at suppressing pain of peripheral origin.

Nerve conduction block induced by high-frequency biphasic electrical current has many potential applications in both clinical medicine and basic neuroscience research [1]-[4]. Understanding the mechanisms underlying this type of nerve block could improve the design of new stimulation waveforms [27][28] and further promote clinical application [29][30]. Simulation analysis using computer models provides a tool to reveal

the possible blocking mechanisms and may help to design new animal experiments to further improve the nerve blocking method.

APPENDIX

The ionic current $I_{i,n}$ at the nth segment is described as:

$$I_{i,n} = g_{Na} m^3 h(V_n - V_{Na}) + g_K n^4 (V_n - V_K) + g_L (V_n - V_L)$$

where g_{Na} (120 $k\Omega^{-1}cm^{-2}$), g_K (36 $k\Omega^{-1}cm^{-2}$) and g_L (0.3 $k\Omega^{-1}cm^{-2}$) are the maximum conductances for sodium, potassium and leakage currents respectively. V_{Na} (115 mV), V_K (-12 mV) and V_L (10.589 mV) are reduced equilibrium membrane potentials for sodium, potassium and leakage ions after substracting the resting membrane potential V_{rest} (-70 mV). m, h, and n are dimensionless variables, whose values always change between 0 and 1. m and h represent activation and inactivation of sodium channels, whereas n represents activation of potassium channels. The evolution equations for m, h, n are the following:

$$dm/dt = \alpha_m (1-m) - \beta_m m$$
$$dh/dt = \alpha_h (1-h) - \beta_h h$$
$$dn/dt = \alpha_n (1-n) - \beta_n n$$

and

$$\alpha_m = \Phi \cdot \frac{2.5 - 0.1V_n}{\exp(2.5 - 0.1V_n) - 1}$$

$$\beta_m = \Phi \cdot 4\exp\left(-\frac{V_n}{18}\right)$$

$$\alpha_h = \Phi \cdot 0.07\exp\left(-\frac{V_n}{20}\right)$$

$$\beta_h = \Phi \cdot \frac{1}{\exp(3 - 0.1V_n) + 1}$$

$$\alpha_n = \Phi \cdot \frac{0.1(1 - 0.1V_n)}{\exp(1 - 0.1V_n) - 1}$$

$$\beta_n = \Phi \cdot 0.125\exp\left(-\frac{V_n}{80}\right)$$

$$\Phi = 3^{(T-6.3)/10}$$

where T is temperature (18.5°C). The initial values for m, h and n (when V_n = 0 mV) are 0.053, 0.596 and 0.318 respectively.

ACKNOWLEDGEMENTS

This study is supported by the NIH under grants DK-068566, DK-090006, DK-091253, and by DOD under grant W81XWH-11-1-0819.

REFERENCES

[1] M. Camilleri, J. Toouli, M.F. Herrera, L. Kow, J.P. Pantoja, C.J. Billington, K.S. Tweden, R.R. Wilson, F.G. Moody, "Selection of electrical algorithms to treat obesity with intermittent vagal block using an implantable medical device," Surg. Obes. Relat. Dis., vol. 5, pp. 224-230, 2009.

[2] J.J. Wattaja, K.S. Tweden, C.N. Honda, "Effects of high frequency alternating

current on axonal conduction through the vagus nerve," J. Neural Eng., vol.8, 056031, 2011.

[3] C. Tai, J.R. Roppolo, W.C. de Groat, "Block of external urethral sphincter contraction by high frequency electrical stimulation of pudendal nerve," J. Urol., vol. 172, pp. 2069–2072, 2004.

[4] B. S. Nashold, J. L. Goldner, J. B.Mullen, D. S. Bright, "Long-term pain control by direct peripheral-nerve stimulation," *J. Bone Joint Surg.*, vol. 64A, pp. 1–10, 1982.

[5] D.M. Ackermann, N. Bhadra, M. Gerges, P.J. Thomas, "Dynamics and sensitivity analysis of high-frequency condition block," J. Neural Eng., vol. 8, pp. 1-14, 2011.

[6] X. Zhang, J.R. Roppolo, W.C. de Groat, C. Tai, "Mechanism of nerve conduction block induced by high- frequency biphasic electrical currents," IEEE Trans. Biomed. Eng., vol. 53, pp. 2445–2454, 2006.

[7] C. Tai, W.C. de Groat, J.R. Roppolo, "Simulation analysis of conduction block in unmyelinated axons induced by high-frequency biphasic electrical currents," IEEE Trans. Biomed. Eng., vol. 52, pp. 1323–1332, 2005.

[8] H. Liu, J.R. Roppolo, W.C. de Groat, C. Tai, "The Role of slow potassium current in nerve conduction block induced by high-frequency biphasic electrical current," IEEE Trans. Biomed. Eng., vol. 56, pp. 137-146, 2009.

[9] N. Bhadra, E. Lahowetz, S. Foldes, K. Kilgore, "Simulation of high-frequency sinusoidal electrical block of mammalian myelinated axons," J. Comput. Neurosci., vol. 22, pp. 313–326, 2007.

[10] N. Bhadra and K. Kilgore, "High-frequency electrical conduction block of mammalian peripheral motor nerve," Muscle Nerve, vol. 32, pp. 782–790, 2005.

[11] R.A. Graunt and A. Prochazka, "Transcutaneously coupled, high-frequency electrical stimulation of the pudendal nerve blocks external urethral sphincter contractions," Neurorehab. Neural Repair, vol. 23, pp. 615-626, 2009.

[12] L. Joseph and R. Butera, "Unmyelinated aplysia nerves exhibit a nonmonotonic blocking response to high-frequency stimulation," IEEE Trans. Neural Syst. Rehab. Eng., vol. 17, pp. 537–544, 2009.

[13] L. Joseph and R. Butera, "High-frequency stimulation selectively blocks different types of fibers in frog sciatic nerve," IEEE Trans. Neural Syst. Rehab. Eng., vol. 19, pp. 550–557, 2009.

[14] A. L. Hodgkin and A. F. Huxley, "A quantitative description of membrane current and its application to conduction and excitation in nerve," *J. Physiol. (Lond.)*, vol. 117, pp. 500–544, 1952.

[15] F. Rattay and M. Aberham, "Modeling axon membranes for functional electrical stimulation," IEEE Trans. Biomed. Eng., vol. 40, pp. 1201-1209, 1993.

[16] F. Rattay, "Analysis of models for extracellular fiber stimulation," IEEE Trans. Biomed. Eng., vol. 36, pp. 676-682, 1989.

[17] W.E. Boyce and R.C. Diprima, "Elementary Differential Equations and Boundary Value Problems," John Wiley & Sons, Inc., 6th ed., pp.436-457, 1997.

[18] C. Tai, W.C. de Groat, J.R. Roppolo, "Simulation of nerve block by high-frequency

sinusoidal electrical current based on the Hodgkin-Huxley model," IEEE Trans. Neural Syst. Rehab. Eng., vol. 13, pp.415–422, 2005.

[19] B. R. Bowman and D. R. McNeal, "Response of single alpha motoneurons to high-frequency pulse train: Firing behavior and conduction block phenomenon," Appl. Neurophysiol., vol. 49, pp. 121–138, 1986.

[20] J. Reboul and A. Rosenblueth, "The action of alternating currents upon the electrical excitability of nerve," Am. J. Physiol. vol. 125, pp. 205–215, 1939.

[21] A. Rosenblueth and J. Reboul, "The blocking and deblocking effects of alternating currents on nerve," Am. J. Physiol., vol. 125, pp. 251–264, 1939.

[22] B. Frankenhaeuser, "Quantitative description of sodium currents in myelinated nerve fibres of xenopus laevis," J. Physiol, vol. 151, pp. 491-501, 1960.

[23] C. Tai, D. Guo, J. Wang, J.R. Roppolo, W.C. de Groat, "Mechanism of conduction block in amphibian myelinated axon induced by biphasic electrical current at ultra-high frequency," J. Comput. Neurosci, vol. 31, pp. 615-623, 2011.

[24] D.M. Ackermann, E.L. Foldes, N. Bhadra, K.L. Kilgore, "Nerve conduction block using combined thermoelectric cooling and high frequency electrical stimulation," J. Neurosci. Methods, vol. 193, pp. 72-76, 2010.

[25] D.M. Ackermann, N. Bhadra, E.L. Foldes, K.L, Kilgore, "Conduction block of whole nerve without onset firing using combined high frequency and direct current," Med. Biol. Eng. Comput., vol. 49, pp. 241-251, 2011.

[26] M. Gerges, E.L. Foldes, D.M. Ackermann, N. Bhadra, N. Bhadra, K.L. Kilgore,

"Frequency and amplitude-transitioned waveforms mitigate the onset response in high-frequency nerve block," J. Neural Eng., vol. 7. pp. 1-9, 2010.

[27] B.J. Roth, "Mechanisms for electrical stimulation of excitable tissue," Critical Rev. Biomed. Eng., vol. 22, pp. 253-305, 1994.

[28] B.J. Roth, "A mathematical model of make and break electrical stimulation of cardiac tissue by a unipolar anode or cathode," IEEE Trans. Biomed. Eng., vol. 42, pp. 1174-1184, 1995.

[29] G.E. Leob, "Neural prosthetic interfaces with the nervous system," Trends Neurosci., vol. 12, pp. 195-201, 1989.

[30] D. Song, G. Raphael, N. Lan, G.E. Loeb, "Computationally efficient models of neuromuscular recruitment and mechanics," J Neural Eng., vol. 5, pp. 175-184, 2008.

FIGURE CAPTIONS

Fig.1. Unmyelinated axon model to simulate conduction block induced by high-frequency biphasic electrical current. The unmyelinated axon is segmented into many small cylinders of length Δx, each of which is modeled by a resistance-capacity circuit based on the Hodgkin–Huxley model. *Ra*: Axoplasm resistance. *Rm*: Membrane resistance. *Cm*: Membrane capacitance. *Va*: Intracellular potential. *Ve*: Extracellular potential.

Fig.2. Blocking the propagation of action potentials along an unmyelinated axon by high-frequency biphasic stimulation at different current intensities. High-frequency (80

kHz) stimulation is continuously delivered at the block electrode. An action potential is initiated via the test electrode at 5 ms after starting the high-frequency stimulation, which is propagating towards both ends of the axon. (a). The 80 kHz stimulation blocks the nerve conduction at the intensity of 45 mA; (b) Conduction is not blocked by the 80 kHz stimulation at 44 mA. The short arrows mark the locations of test and block electrodes along the axon. The white arrow indicates the propagation of an action potential. Axon diameter: 1μm.

Fig.3. The intensity threshold to block nerve conduction changes with the stimulation frequency. The block threshold peaks at 13-16 kHz for axons of diameters between 1-2 μm and then gradually decreases as the frequency increases above 20 kHz.

Fig.4. The changes in membrane potentials, ionic currents and activation/inactivation of ion channels near the block electrode when conduction block occurs as shown in Fig.2 (a). The legends in (a) indicate the distance of each axon segment to the block electrode. Node at 0 mm is under the block electrode. Axon diameter: 1μm. (a) Change of membrane potentials, (b) Na+ current, (c) K+ current, (d) Na+ channel activation, (e) Na+ channel inactivation, (f) K+ channel activation.

Fig.5. The state of ion channel under the block electrode changes with stimulation frequency at the blocking threshold intensity. (a) Na+ channel activation, (b) Na+ channel inactivation, (c) K+ channel activation. The Na+ channel is completely closed (m=0) when the frequency is greater than 20 kHz. Axon diameter: 1 μm.

Fig.6. Ion channel activation/inactivation under the block electrode changing with

stimulation intensity (a)-(c) at 80 kHz frequency or changing with stimulation frequency (d)-(f) at 45 mA intensity. Axon diameter: 1 μm. Block threshold is at 80 kHz and 45 mA as indicated by the arrow in (a) and (d).

Fig.7. Change of membrane potential induced by high-frequency stimulation in a passive axon without sodium and potassium channels. Axon diameter: 1μm. (a) Change of membrane potential induced by high-frequency stimulation (80 kHz, 45 mA) after the stimulation was on for 5.9894 ms, (b) Difference between membrane potentials under the block electrode induced by high-frequency stimulation (80 kHz, 45 mA) in axons with passive or active membrane properties, (c) The passive axon membrane under the block electrode is hyperpolarized to about -98 mV [(-28 mV) + (-70 mV resting potential)] by stimulation of different frequencies (40-100 kHz) at their corresponding block thresholds (91-36 mA).

Fig.8. Initial action potential induced by high-frequency stimulation at the block threshold intensity changes with stimulation frequency. (a) 20 kHz stimulation at block threshold intensity induces an initial action potential. (b) 40 KHz stimulation at block threshold intensity does not induce an initial action potential. Axon diameter: 1 μm.

Fig.9. The initial transient state of the ion channels under the block electrode induced by high-frequency stimulation at the blocking threshold intensity. (a) Na+ channel activation, (b) Na+ channel inactivation, (c) K+ channel activation. The Na+ channel is quickly driven into a completely closed state ($m \approx 0$) when the frequency is greater than 40 kHz. Axon diameter: 1 μm.

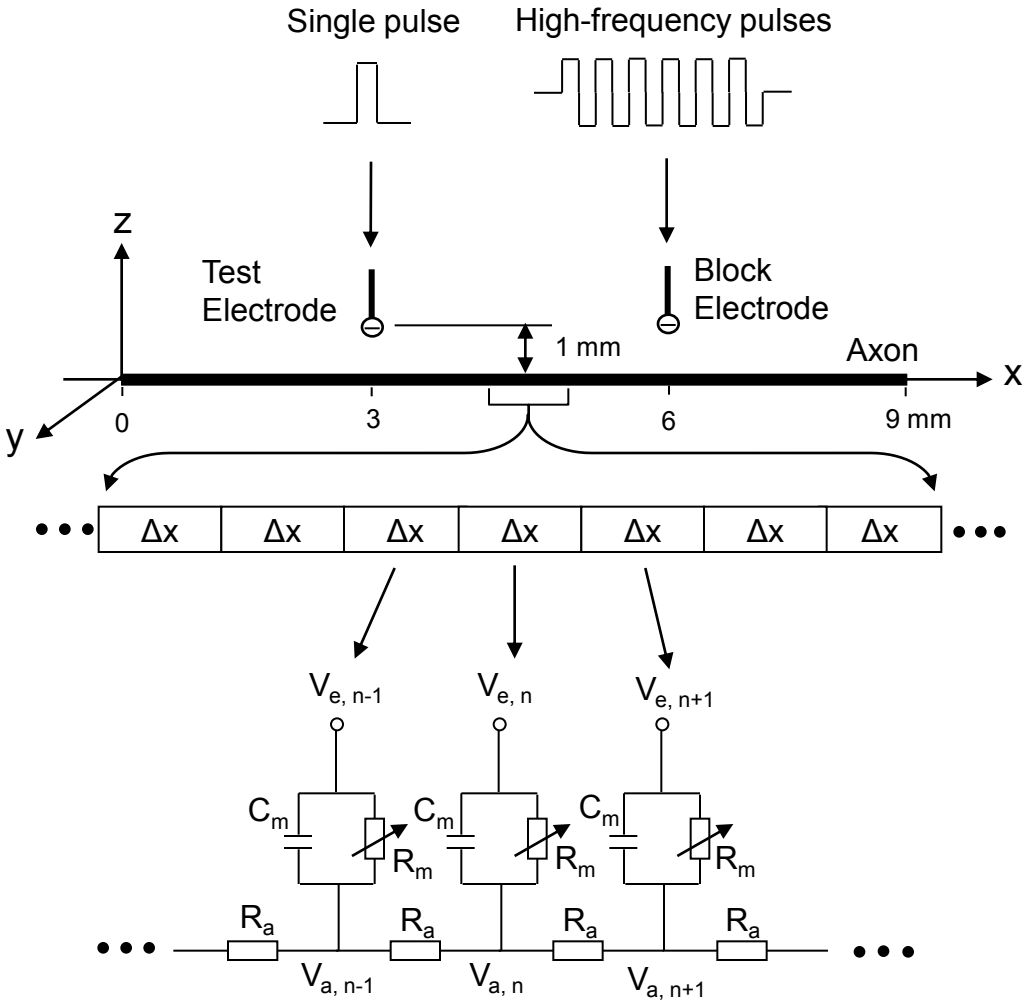

Fig.1. Unmyelinated axon model to simulate conduction block induced by high-frequency biphasic electrical current. The unmyelinated axon is segmented into many small cylinders of length Δx, each of which is modeled by a resistance-capacity circuit based on the Hodgkin–Huxley model. R_a: Axoplasm resistance. R_m: Membrane resistance. C_m: Membrane capacitance. V_a: Intracellular potential. V_e: Extracellular potential.

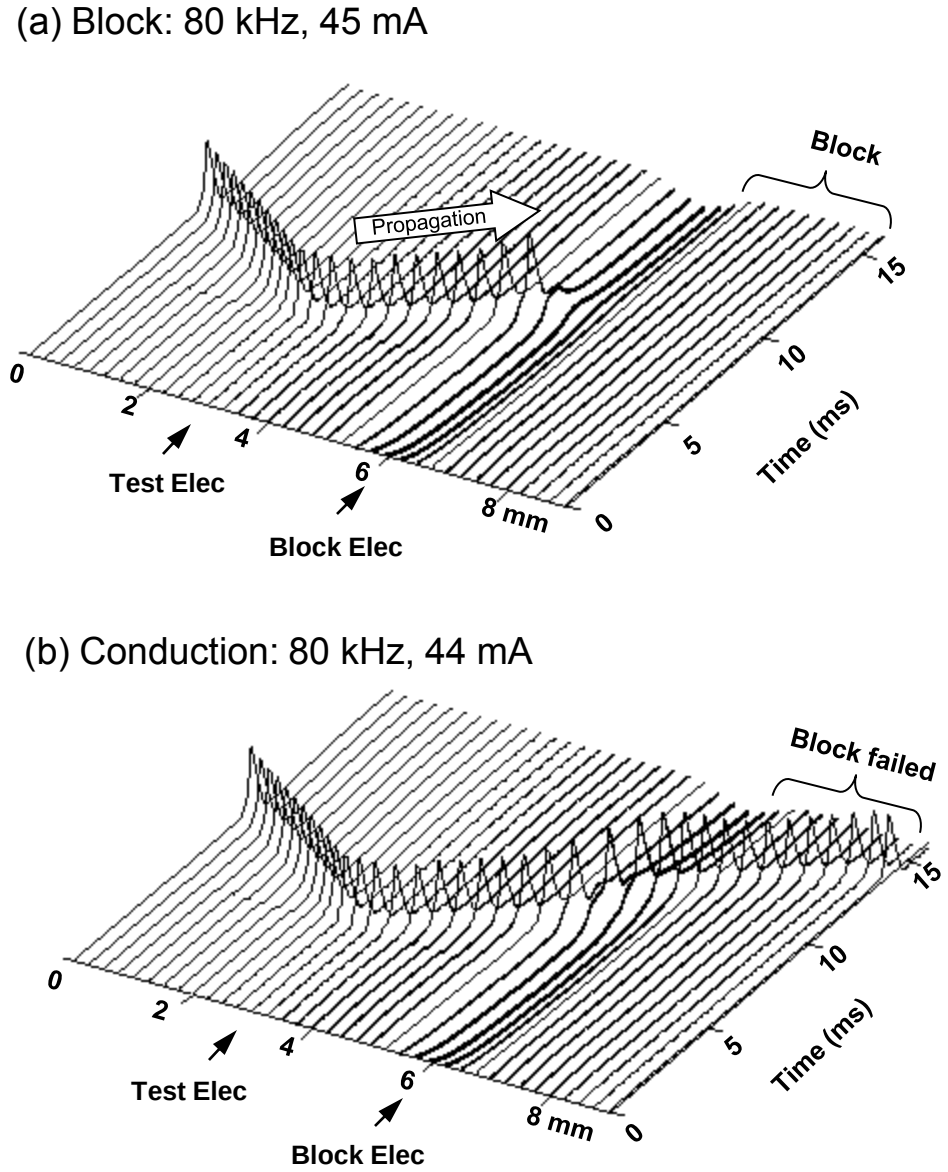

Fig.2. Blocking the propagation of action potentials along an unmyelinated axon by high-frequency biphasic stimulation at different current intensities. High-frequency (80 kHz) stimulation is continuously delivered at the block electrode. An action potential is initiated via the test electrode at 5 ms after starting the high-frequency stimulation, which is propagating towards both ends of the axon. (a). The 80 kHz stimulation blocks the nerve conduction at the intensity of 45 mA; (b) Conduction is not blocked by the 80 kHz stimulation at 44 mA. The short arrows mark the locations of test and block electrodes along the axon. The white arrow indicates the propagation of an action potential. Axon diameter: 1μm.

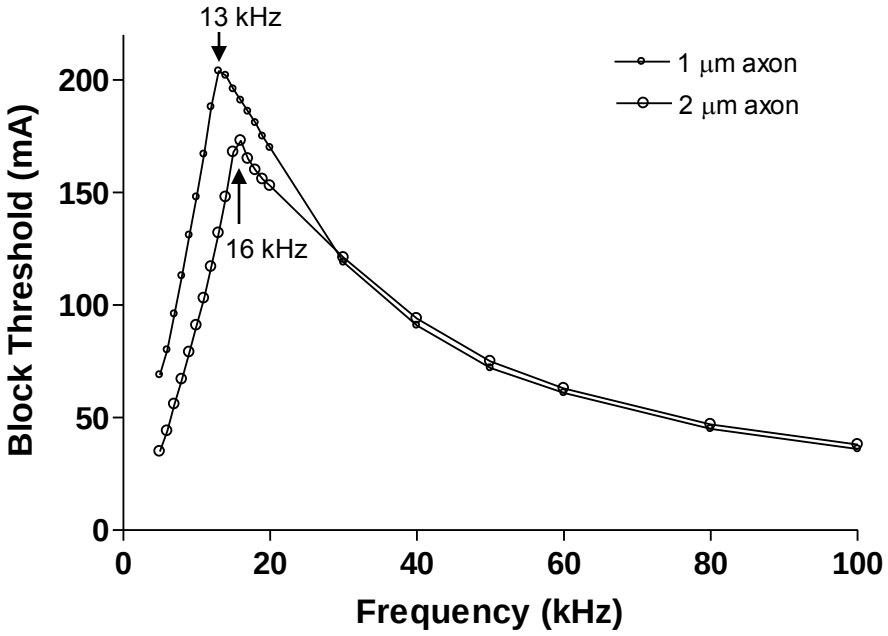

Fig.3. The intensity threshold to block nerve conduction changes with the stimulation frequency. The block threshold peaks at 13-16 kHz for axons of diameters between 1-2 μm and then gradually decreases as the frequency increases above 20 kHz.

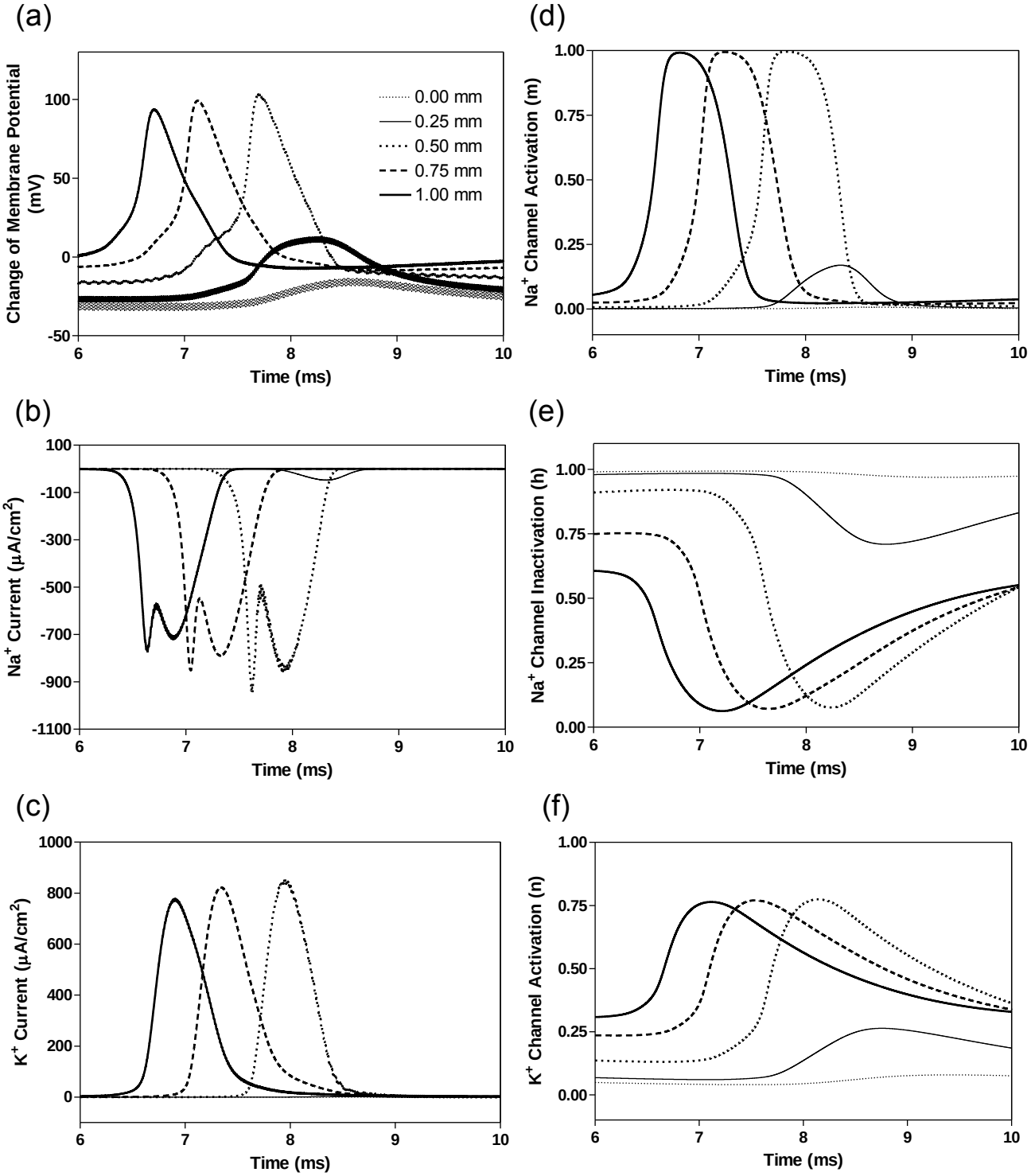

Fig.4. The changes in membrane potentials, ionic currents and activation/inactivation of ion channels near the block electrode when conduction block occurs as shown in Fig.2 (a). The legends in (a) indicate the distance of each axon segment to the block electrode. Node at 0 mm is under the block electrode. Axon diameter: 1μm. (a) Change of membrane potentials, (b) Na^+ current, (c) K^+ current, (d) Na^+ channel activation, (e) Na^+ channel inactivation, (f) K^+ channel activation.

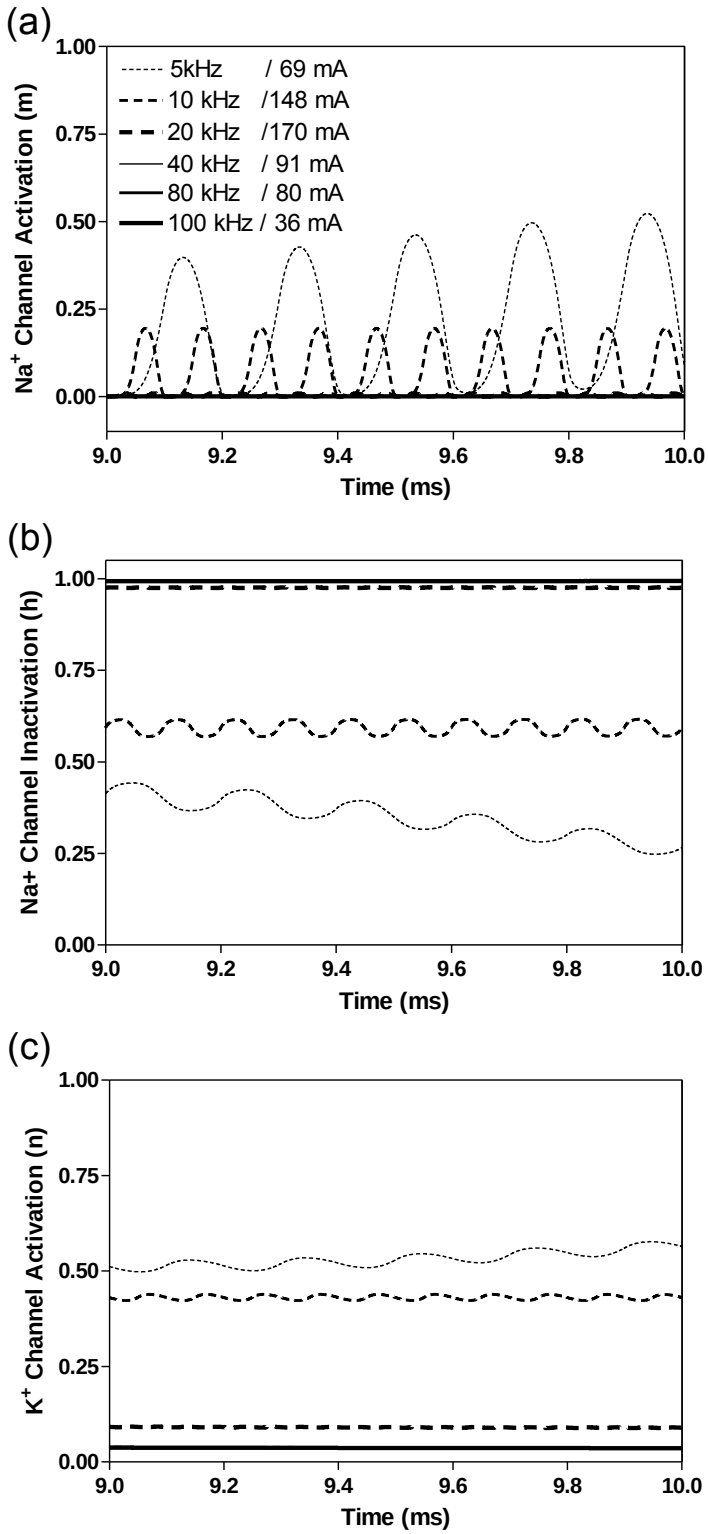

Fig.5. The state of ion channel under the block electrode changes with stimulation frequency at the blocking threshold intensity. (a) Na^+ channel activation, (b) Na^+ channel inactivation, (c) K^+ channel activation. The Na^+ channel is completely closed (m=0) when the frequency is greater than 20 kHz. Axon diameter: 1 μm.

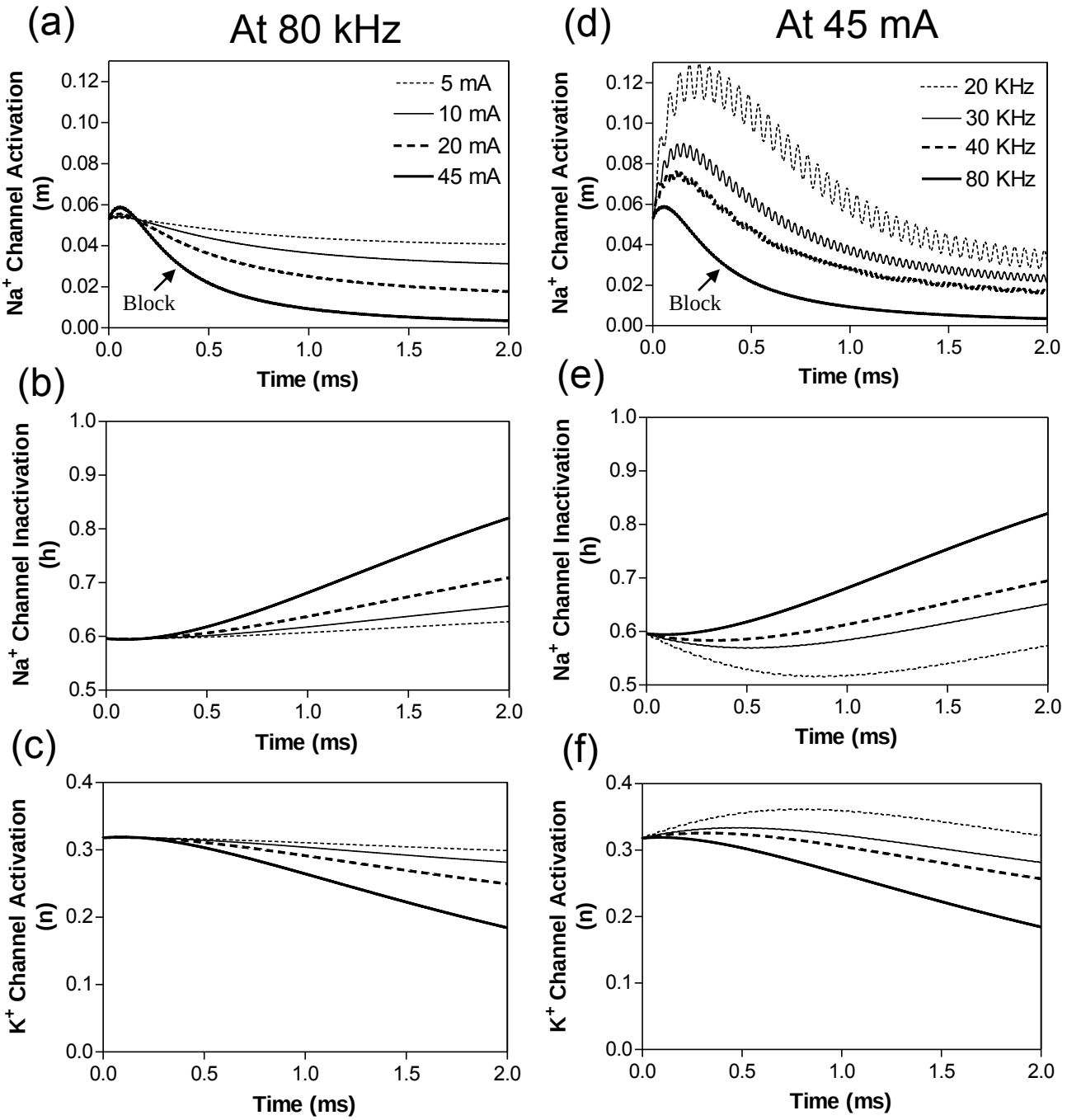

Fig.6. Ion channel activation/inactivation under the block electrode changing with stimulation intensity (a)-(c) at 80 kHz frequency or changing with stimulation frequency (d)-(f) at 45 mA intensity. Axon diameter: 1 μm. Block threshold is at 80 kHz and 45 mA as indicated by the arrow in (a) and (d).

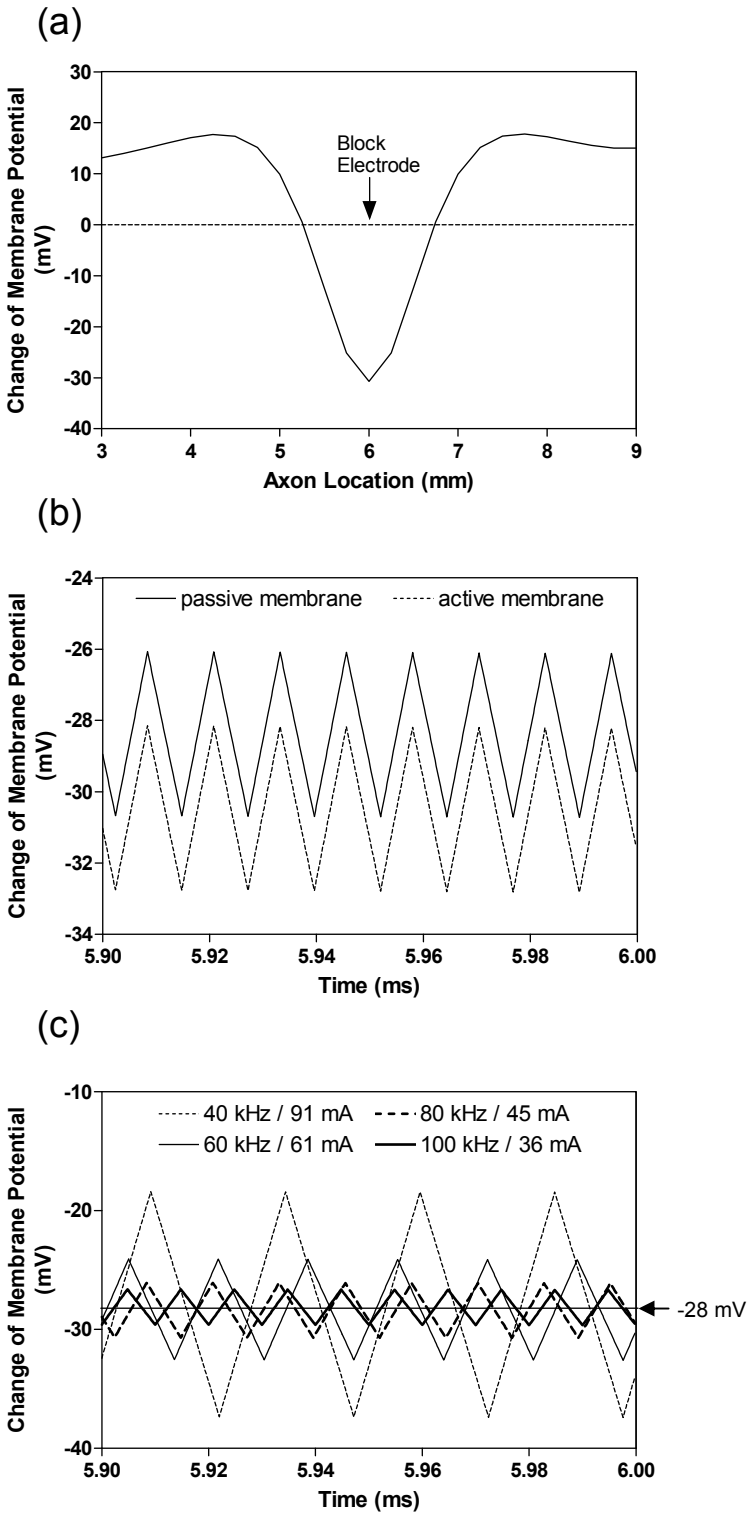

Fig.7. Change of membrane potential induced by high-frequency stimulation in a passive axon without sodium and potassium channels. Axon diameter: 1 μm. (a) Change of membrane potential induced by high-frequency stimulation (80 kHz, 45 mA) after the stimulation was on for 5.9894 ms, (b) Difference between membrane potentials under the block electrode induced by high-frequency stimulation (80 kHz, 45 mA) in axons with passive or active membrane properties, (c) The passive axon membrane under the block electrode is hyperpolarized to about -98 mV [(-28 mV) + (-70 mV resting potential)] by stimulation of different frequencies (40-100 kHz) at their corresponding block thresholds (91-36 mA).

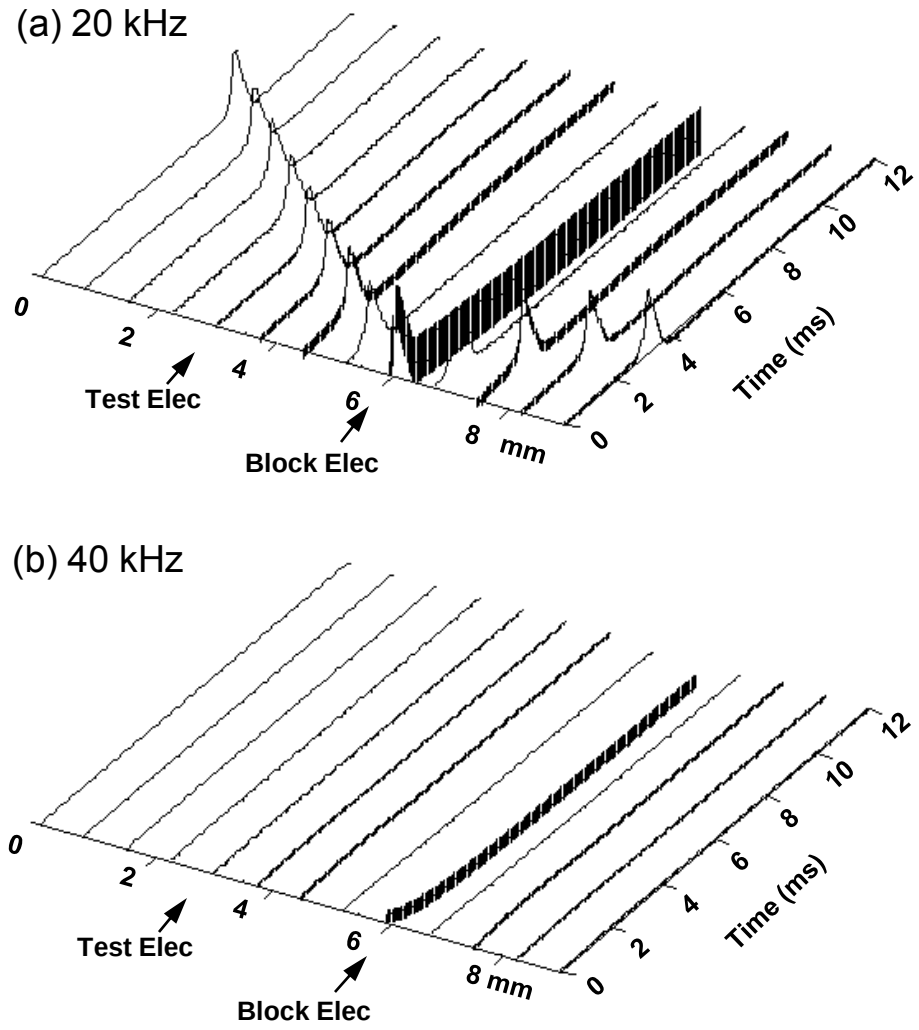

Fig.8. Initial action potential induced by high-frequency stimulation at the block threshold intensity changes with stimulation frequency. (a) 20 kHz stimulation at block threshold intensity induces an initial action potential. (b) 40 KHz stimulation at block threshold intensity does not induce an initial action potential. Axon diameter: 1 μm.

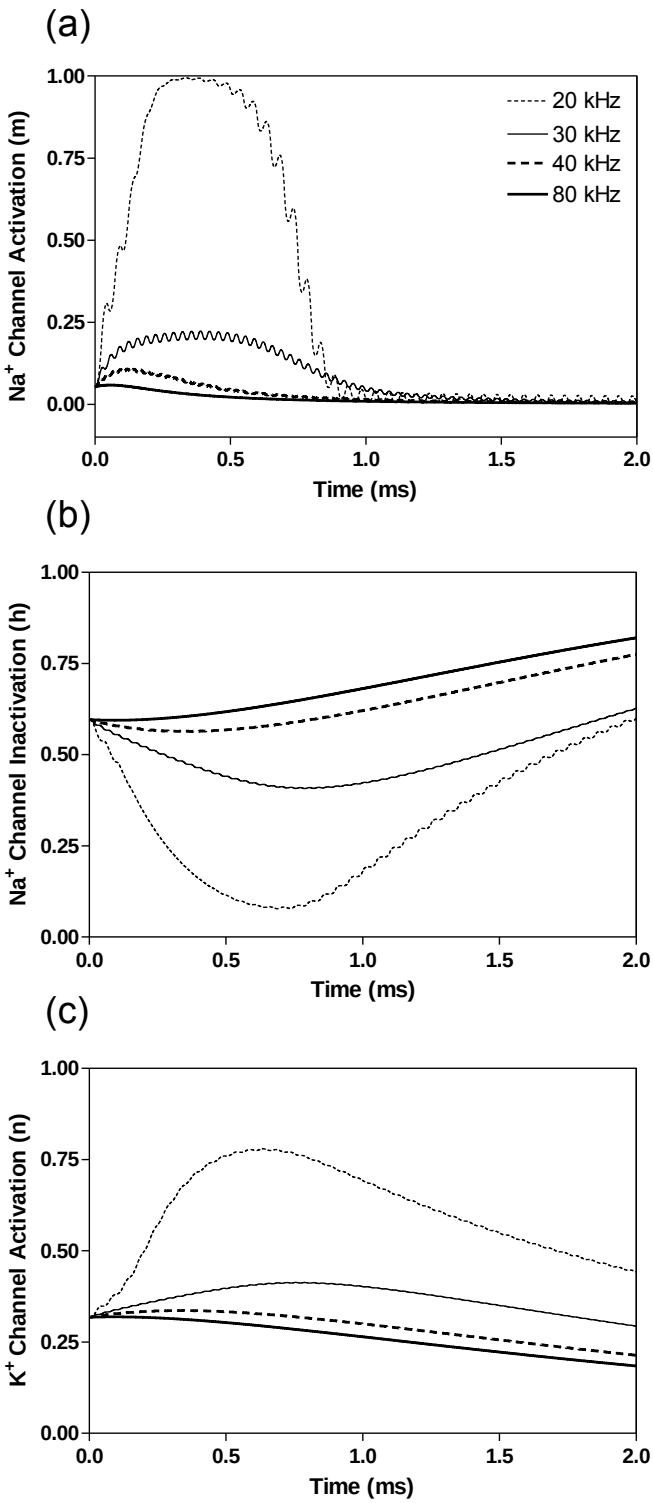

Fig.9. The initial transient state of the ion channels under the block electrode induced by high-frequency stimulation at the blocking threshold intensity. (a) Na^+ channel activation, (b) Na^+ channel inactivation, (c) K^+ channel activation. The Na^+ channel is quickly driven into a completely closed state ($m \approx 0$) when the frequency is greater than 40 kHz. Axon diameter: 1 μm.

Non-monotonic Block of Conduction in Myelinated Axons by High-Frequency Biphasic Electrical Stimulation

Shouguo Zhao [1,2], Jicheng Wang [1], James R. Roppolo [3],
William C. de Groat [3], Changfeng Tai [1]

[1] Department of Urology, University of Pittsburgh, Pittsburgh, PA
[2] Department of Biomedical Engineering, Beijing Jiaotong University, P.R. China
[3] Department of Pharmacology and Chemical Biology, University of Pittsburgh, PA

Correspondence to:

Changfeng Tai, Ph.D.
Department of Urology
University of Pittsburgh
700 Kaufmann Building
Pittsburgh, PA15213, USA
Phone: 412-692-4142
Fax: 412-692-4380
Email: cftai@pitt.edu

ABSTRACT

This study used the Frankenhaeuser–Huxley axonal model to simulate nerve conduction block in myelinated axons during high-frequency (10-300 kHz) biphasic electrical stimulation. The analysis revealed a non-monotonic relationship between the minimal intensity of stimulation to produce conduction block (termed block threshold) and stimulation frequency. Block threshold increases as frequency increases up to a certain level which varies with axonal diameter and then the block threshold decreases as frequency increases further. The results indicate that complete deactivation of sodium and potassium channels by the high-frequency stimulation is the mechanism underlying the decrease in block threshold. This nerve blocking mechanism has the potential to eliminate the action potentials elicited at the beginning of blocking stimulation. Although the non-monotonic block response in myelinated axons still needs to be confirmed in animal studies, a similar non-monotonic block response has been observed in unmyelinated axons of sea slugs and frogs. This simulation study further increases our understanding of conduction block in myelinated axons induced by high-frequency biphasic electrical stimulation, and can guide future animal experiments as well as optimize stimulation parameters that might be used for electrically induced nerve block in clinical applications.

Key Words: nerve, block, simulation, high-frequency, model.

I. INTRODUCTION

High-frequency (kHz) biphasic electrical stimulation has recently been investigated extensively due to its potential clinical application to block peripheral nerve conduction (Camilleri et al. 2009; Nashold et al. 1982; Tai et al. 2004; Wattaja et al. 2011). Although the mechanisms underlying this nerve block are still unclear (Ackermann et al. 2011; Zhang et al. 2006), previous animal studies of myelinated axons have shown that the block threshold intensity monotonically increases as the stimulation frequency increases up to 50 kHz (Bhadra and Kilgore 2005; Graunt and Prochazka 2009; Joseph and Butera 2011). Our recent computer simulation study of large (10-20 μm diameter) myelinated axons further indicates a monotonic increase in block threshold up to 100 kHz (Tai et al. 2011). However, recent animal studies (Joseph and Butera 2009, 2011) revealed that this monotonic relationship does not hold in unmyelinated axons where the block threshold intensity only increases with frequency up to about 12-15 kHz and then decreases as the stimulation frequency further increases. This discovery raises the question about what causes the difference of high-frequency block between myelinated and unmyelinated axons. Answering this question will help to understand the mechanisms underlying nerve conduction block induced by high-frequency biphasic electrical stimulation.

Due to the difficulties in recording ion channel activity in axonal nodes during high-frequency biphasic electrical stimulation, the mechanisms of nerve block have been mainly investigated by modeling and computer simulation (Ackermann et al. 2011; Bhadra et al. 2007; Liu et al. 2009; Tai et al. 2005a,b, 2009, 2011; Zhang et al. 2006).

These simulation studies have been successful in reproducing many phenomena observed in animal experiments, for example the minimal block frequency, the influence of temperature on minimal block frequency, and the relationship between axon diameter and block threshold. The newly discovered non-monotonic relationship between block threshold and stimulation frequency was also successfully reproduced in our recent simulation study of unmyelinated axons (Zhao et al. 2012). This study indicates that the monotonic decrease in block threshold in unmyelinated axons at frequencies above 15 kHz is due to a complete deactivation of sodium and potassium channels by the high-frequency (>15 kHz) biphasic stimulation, which causes the axonal membrane to become a passive membrane resulting in failure to conduct action potentials.

Although our recent simulation study (Tai et al. 2011) of large (10-20 um diameter) myelinated axons showed a monotonic increase in block threshold with stimulation frequency up to 100 kHz, the blocking mechanism changes from a constant activation of potassium channels by high-frequency stimulation at 4-10 kHz to a constant activation of sodium channels at frequencies of 20-100 kHz. This change of blocking mechanism is due to the fact that sodium channel has a faster kinetics than potassium channel. Therefore, as the frequency increases the stimulation first drives the potassium channel to be constantly open before it drives the sodium channel to be constantly open. These differences in channel kinetics raise the possibility that the sodium and/or potassium channels in myelinated axons could be driven to a completely deactivated state if the stimulation frequency is increased above 100 kHz, resulting in a monotonic decrease in

block threshold at frequencies above 100 kHz similar to what happens in unmyelinated axons at frequencies above 15 kHz. It is known that the ion channel kinetics of myelinated axons is faster than unmyelinated axons (Frankenhaeuser 1960; Hodgkin and Huxley 1952). Therefore, it is reasonable to expect that a higher frequency would be required in myelinated axons than in unmyelinated axons to drive the sodium and/or potassium channels to completely deactivated states.

In this study we employed a myelinated axonal model (Frankenhaeuser–Huxley model) (Frankenhaeuser and Huxley 1964; Ratty 1998; Ratty and Aberham 1993) to simulate nerve block and to determine: (1) if a decrease in block threshold can be produced at frequencies above 100 kHz; (2) what happens to the sodium and potassium channels when this decrease in block threshold occurs. Understanding the mechanisms of nerve conduction block induced by high-frequency biphasic electrical stimulation will be very useful in developing new nerve blocking methods, optimizing stimulation parameters, or improving the efficacy of blocking nerves in different clinical applications.

II. METHODS

The myelinated axon model used in our study is showed in Fig.1. A 40 mm long, myelinated axon is modeled with the inter-node length $\Delta x=100d$ (d is the myelinated axon diameter). Each node (nodal length: L=2.5 um) is modeled by a membrane capacitance (C_m) and a variable membrane resistance (R_m). The ionic currents passing through the variable membrane resistance are described by Frankenhaeuser–Huxley

equations (Frankenhaeuser and Huxley 1964; Ratty 1998; Ratty and Aberham 1993). Two monopolar point electrodes (with the indifferent electrode at infinity) are placed at 1 mm distance from the axon. One is the block electrode at the 30 mm location along the axon, where the high frequency biphasic current is delivered (Fig.1). The other is the test electrode at 10 mm location, which delivers a uniphasic single pulse (pulse width 0.1 ms and intensity 0.5-2mA) to evoke an action potential and test whether this action potential can propagate through the site of the block electrode. The test electrode is always the cathode (negative pulse), and the block electrode delivers a biphasic pulse with the cathodal phase first.

We assume that the myelinated axon is in an infinite homogeneous medium (resistivity $\rho_e = 300\ \Omega\text{cm}$). After neglecting the small influence of the axon in the homogeneous medium, the extracellular potential $V_{e,n}$ at the nth node along the axon can be described by:

$$V_{e,n} = \frac{\rho_e}{4\pi}\left[\frac{I_{block}(t)}{\sqrt{(n\Delta x - x_0)^2 + z_0^2}} + \frac{I_{test}(t)}{\sqrt{(n\Delta x - x_1)^2 + z_1^2}}\right]$$

where $I_{block}(t)$ is the high-frequency biphasic current delivered to the block electrode (at location x_0 = 30 mm, z_0 = 1 mm); $I_{test}(t)$ is the single test pulse delivered to the test electrode (at location x_1 = 10 mm, z_1 = 1 mm).

The change of the membrane potential V_n at the nth node of the myelinated axon is described by:

$$\frac{dV_n}{dt} = \left[\frac{d\Delta x}{4\rho_i L} \left(\frac{V_{n-1} - 2V_n + V_{n+1}}{\Delta x^2} + \frac{V_{e,n-1} - 2V_{e,n} + V_{e,n+1}}{\Delta x^2} \right) - I_{i,n} \right] / c_m$$

where $V_n = V_{a,n} - V_{e,n} - V_{rest}$; $V_{a,n}$ is the intracellular potential at the nth node; $V_{e,n}$ is the extracellular potential at the nth node; V_{rest} is the resting membrane potential; ρ_i is the resistivity of axoplasm (100 Ωcm); c_m is the capacity of the membrane (2 uF/cm^2); $I_{i,n}$ is the ionic current at the nth node described by Frankenhaeuser–Huxley equations (Frankenhaeuser and Huxley 1964; Ratty 1998; Ratty and Aberham 1993) (see appendix).

The myelinated axon model was solved by Runge-Kutta method (Boyce and Diprima 1997) with a time step of 0.5 μsec. The simulation was always started at initial condition $V_n = 0$. The membrane potentials at the two end nodes of the modeled axon were always equal to the membrane potentials of their closest neighbors, which implemented sealed boundary conditions (no longitudinal currents) at the two ends of the modeled axon. The block threshold intensity was determined with a resolution of 0.1 mA. The simulation was performed for myelinated axons of different diameters (2, 5, 10 and 20 μm) with the temperature parameter set at 37 °C.

III. RESULTS

A. Non-monotonic block of conduction in myelinated axons

Fig.2 shows that the Frankenhaeuser–Huxley model can successfully simulate the conduction block induced by high-frequency (120 kHz) biphasic electrical stimulation in a myelinated axon of 2 μm diameter. In Fig.2 (a) the 120 kHz blocking stimulation (19.2

mA) hyperpolarizes [also see Fig.4 (a)] the axon membrane at the block electrode without generating initial action potentials. At 5 ms after the start of blocking stimulation, the test electrode delivers a single pulse that generates another action potential propagating toward the block electrode [see the white arrow in Fig.2 (a)]. This action potential fails to propagate through the region of the block electrode due to the presence of the high-frequency biphasic electrical stimulation. However, at a lower stimulation intensity [19.1 mA in Fig.2 (b)] the 120 kHz stimulation does not block nerve conduction and the action potential propagates through the site of block electrode.

Fig.3 shows the intensity threshold for inducing conduction block at different frequencies (10-300 kHz) for myelinated axons of different diameters (2-20 μm). The block threshold increases initially and then decreases with increasing stimulation frequency, showing a non-monotonic relationship between block threshold and stimulation frequency. The block threshold peaks at different frequencies (80-250 kHz) for axons of different diameters (2-20 μm). The peak frequency is higher for a larger diameter axon.

B. Mechanism underlying the non-monotonic block response

In order to understand why the block threshold starts to decrease when the stimulation frequency is greater than a certain value (80-250 kHz) for an axon of a certain diameter (2-20 μm) (Fig.3), we further investigated the changes in membrane potential, ionic currents, and activation/inactivation of the sodium and potassium channels along the

myelinated axons at different nodes near the block electrode. Fig.4 shows the same simulation as in Fig.2 (a) for the 2 μm diameter axon including more detailed information for the 4 consecutive axon nodes at distances of 0-1.2 mm from the block electrode (the node at 0 mm is under the block electrode) during blocking stimulation of 120 kHz.

At axon nodes approaching the block electrode, the amplitude of action potential greatly declined [Fig.4 (a)]. Action potential propagation completely stopped at the node (0 mm) under the block electrode, where the axon membrane is hyperpolarized to about -120 mV [(-50 mV) + (-70 mV resting potential), see Fig.4 (a)] and a very small sodium current [Fig.4 (b)] and no potassium current [Fig.4 (c)] are generated by the in-coming action potential. The behavior of the action potential and ionic currents can be explained by the activation/inactivation of the sodium and potassium channels as shown in Fig.4 (d)-(f). As the action potential propagates toward the block electrode, the activation (m) of sodium channels significantly declines at the node under the block electrode (0 mm) [Fig.4 (d)]. Meanwhile, inactivation (h) of sodium channels is minimal (>0.7) at the node (0 mm) under the block electrode [Fig.4 (e)]. The combination of activation (m) and inactivation (h) of sodium channels [Fig.4 (d) and (e)] determines that the amplitude of sodium current is minimal at the node (0 mm) under the block electrode [Fig.4 (b)]. Therefore the conduction block is due to a significant deactivation of the sodium channels under the block electrode [Fig.4 (d)]. The same blocking mechanism is observed in axons of different diameters (2-20 μm) when stimulation frequency is greater than the corresponding peak threshold frequency (80-250 kHz, see Fig.3).

Meanwhile, the change in potassium activation (n) induced by the in-coming action potential also disappears at the node (0 mm) under the block electrode [Fig.4 (f)] because the potassium channels are also deactivated, which results in no potassium current at this node [Fig4 (c)]. Therefore, 120 kHz stimulation deactivates both sodium and potassium channels at the node under the block electrode.

At the blocking threshold intensity, the effect of different stimulation frequencies on activation and inactivation of sodium and potassium channels at the node under the block electrode is shown in Fig.5 for the 2 μm diameter axon. At the frequency range of 20-80 kHz the sodium channel is constantly open with its activation (m) oscillating between 0.2-0.7 during the blocking stimulation [Fig.5 (a)] while the inactivation (h) is at a level around 0.1 [Fig.5 (b)]. Meanwhile, the potassium channel is also constantly open with its activation (n) around 0.3-0.5 [Fig.5 (c)]. Our previous study (Tai et al. 2011) showed that the constantly opened sodium and potassium channels cause the axon membrane to lose the ability to regulate the ion currents during action potential generation resulting in conduction block. Since a higher stimulation intensity is required for a higher frequency to maintain the ion channels to be constantly open (Tai et al. 2011), a monotonic increase in block threshold was observed at 20-80 kHz for the 2 μm diameter axon (Fig.3).

However, as the stimulation frequency increases above 80 kHz the sodium activation (m) becomes almost zero [i.e., completely deactivated, Fig.5 (a)] while the inactivation (h) is close to one [i.e., minimal inactivation, Fig.5 (b)]. The complete deactivation of sodium channel during high-frequency stimulation becomes the mechanism underlying axonal

conduction block (Fig.4). In addition, potassium channels are also completely deactivated as the frequency increases above 80 kHz [Fig.5 (c)]. Complete deactivation of sodium channels requires a lower stimulation intensity as the frequency increases above 80 kHz [see legends in Fig.5 (b)], thereby resulting in a monotonic decrease in block threshold.

At frequencies above 80 kHz, the high-frequency stimulation must drive the sodium channel to a certain level of deactivation in order to achieve conduction block in the 2 μm diameter axon (Fig. 6). At a specific frequency (120 kHz), a stimulation of higher intensity deactivates the sodium channel more than the stimulation of a lower intensity [Fig.6 (a)]. This explains why a minimal stimulation intensity (i.e. block threshold) is required at a specific frequency to block the nerve conduction (Fig.3). Meanwhile, at a specific stimulation intensity (19.2 mA), stimulation at a higher frequency deactivates the sodium channel more than stimulation at a lower frequency [Fig.6 (d)]. Therefore, in order to deactivate the sodium channels to a level ($m \approx 0$) for inducing a conduction block, the stimulation at a higher frequency requires a lower intensity (Fig.3). At the block threshold (19.2 mA at 120 kHz) the sodium channels are significantly deactivated within 0.3 ms from the beginning of the stimulation [Fig.6 (a)/(d)]. The sodium channel inactivation [Fig.6 (b)/(e)] and the potassium channel activation [Fig.6 (c)/(f)] are also changed significantly during this time period.

C. Response of an axon with passive membrane properties to high-frequency biphasic electrical stimulation

Because our results indicate that both sodium and potassium channels are completely deactivated by high-frequency stimulation, the axonal membrane becomes a passive membrane under the block electrode when the block threshold starts to decrease with increasing frequency. Therefore, it is logical to hypothesize that the decrease in block threshold (see Fig.3) is mainly determined by the passive properties of the axonal membrane. To test this hypothesis we removed both sodium and potassium channels in the Frankenhaeuser–Huxley model but retained the non-specific and leakage ion channels. The responses of this passive axonal model to high-frequency stimulation are presented in Fig.7.

When the high-frequency (120 kHz) stimulation of block threshold intensity (19.2 mA) is applied to the passive axon (2 μm diameter), it hyperpolarizes the axonal membrane under the block electrode (Fig.7 A) and the hyperpolarization oscillates around -115 mV [(-45 mV) + (-70 mV resting potential), see the solid line in Fig.7 B]. The same response is also induced in the active axon (Frankenhaeuser–Huxley model) (see the dashed line in Fig.7 B). This result confirms that the hyperpolarization induced by high-frequency stimulation under the block electrode is mainly due to the passive properties of the axon that becomes a distributed passive resistance-capacitance cable model (see Fig.1).

When stimulations of different frequencies (120-250 kHz) are applied at their block

threshold intensities to the passive axon, they produce a hyperpolarization under the block electrode oscillating around the same potential -110 mV [(-40 mV) + (-70 mV resting potential), see Fig.7 C]. However, a higher frequency requires a lower intensity in order to hyperpolarize the passive membrane to the same membrane potential (see the legends in Fig.7 C). This explains why the block threshold in Fig.3 decreases with the increasing frequency.

In summary, the results from the passive axon model further confirm the hypothesis that the high-frequency stimulation completely closes both sodium and potassium channels under the block electrode (Figs.4-6) causing the axon membrane under the block electrode to be a passive membrane. Therefore, the monotonic decrease in block threshold with increasing frequency (see Fig.3) is mainly determined by the passive properties of the axonal membrane (Fig.7 C).

D. Initial action potential generation by high-frequency biphasic electrical stimulation

At the block thresholds and frequencies below those causing a decrease in block threshold, the high-frequency biphasic stimulation always generates initial action potentials before it blocks nerve conduction (Ackermann et al. 2011; Bhadra et al. 2007; Liu et al. 2009; Tai et al. 2005a,b, 2009, 2011; Zhang et al. 2006). These initial action potentials are also observed at 90 kHz [Fig.8 (a)], but not at 120 kHz [Fig.8 (b)] for a 2 μm diameter axon. This is because at the block thresholds and frequencies above 100 kHz the sodium channels at the node under the block electrode are quickly deactivated

[m≈0, Fig.9 (a)] once the blocking stimulation starts. This quick and complete deactivation of sodium channels eliminates the initiation of any action potentials although sodium inactivation [Fig.9 (b)] and potassium activation [Fig.9 (c)] are only changed slightly at the beginning of high-frequency stimulation. This result further confirms that the complete deactivation of sodium channels is the cause of nerve conduction block because it also blocks the generation of action potential that is supposed to be induced by the high-frequency stimulation at the initiation of the stimulation.

IV. DISCUSSION

This study using the Frankenhaeuser–Huxley axonal model simulated nerve conduction block in myelinated axons during high-frequency (10-300 kHz) biphasic electrical stimulation (Fig.2) and predicted a non-monotonic relationship between block threshold and stimulation frequency (Fig.3). The results revealed a complete deactivation of sodium and potassium channels by the high-frequency stimulation, which is the mechanism underlying the decrease in block threshold (Figs.4-7). A larger axon requires a higher frequency to induce a decrease in block threshold (Fig.3). This nerve blocking mechanism has the potential to eliminate the action potentials elicited at the beginning of blocking stimulation (Figs.8-9). These results have significant implications for future animal experiments and for clinical applications of the nerve block methods.

This study predicts in myelinated axons that the block threshold will reach a peak and then gradually decrease when the stimulation frequency increases above 80 kHz

(Fig.3). Although this prediction still needs to be confirmed by animal studies, a similar non-monotonic block response has been observed in unmyelinated axons of sea slugs and frogs with the block threshold peaks ranging between 12-15 kHz (Joseph and Butera 2009a,b). Previous animal studies that examined block of myelinated axons only tested frequencies up to 50 kHz (Bhadra and Kilgore 2005; Graunt and Prochazka 2009; Joseph and Butera 2011). The present study suggests that higher frequencies (50-300 kHz) should be tested in myelinated axons to block the nerve conduction. One of the advantages of using higher frequencies such as 300 kHz (see Fig.3) to block the myelinated axons is that the initial nerve firing induced by the high-frequency stimulation can be eliminated (see Figs. 8-9), which is very desirable for clinical applications (Camilleri et al. 2009; Gerges et al. 2010; Nashold et al. 1982; Tai et al. 2004; Wattaja et al. 2011).

This study and our previous studies (Tai et al. 2011; Zhang et al. 2006) using the myelinated axonal model (Frankenhaeuser–Huxley model) have revealed several different blocking mechanisms for different stimulation frequencies. These studies indicate that the kinetics of ion channel gating plays a major role in the conduction block induced by high-frequency biphasic electrical stimulation. The kinetics of the potassium channel is slow compared to the sodium channel (Frankenhaeuser 1960; Hodgkin and Huxley 1952), and therefore this channel does not follow high-frequencies very well. Thus the potassium channel becomes constantly open as the frequency increases to the minimal blocking frequency of about 4 kHz (Liu et al. 2009; Zhang et al. 2006). This

potassium channel opening mechanism governs the monotonic increase in block threshold at the frequency range of 4-10 kHz (Liu et al. 2009; Zhang et al. 2006). As the frequency increases further (>20 kHz), it saturates the faster kinetics of the sodium channel causing the channel to be constantly open and lose its ability to regulate sodium current during action potential generation resulting in a conduction block (Tai et al. 2011). This sodium channel opening mechanism governs the monotonic increase in block threshold from 20 kHz to the frequency at which the block threshold peaks (Tai et al. 2011). Further increasing the stimulation frequency above the peak threshold frequency will completely deactivate both sodium and potassium channels [Figs.4-6] causing the axon membrane to become passive (Fig.7) and conduction to fail (Fig.2). This sodium and potassium channel deactivation mechanism is responsible for the monotonic decrease in block threshold (Figs.2-7). These ion channel kinetic mechanisms are supported by evidence from animal studies that the minimal blocking frequency is about 4 kHz (Bowman and McNeal 1986; Reboul and Rosenblueth 1939; Rosenblueth and Reboul 1939) and that the block threshold monotonically increases in the frequency range of 4-50 kHz (Bhadra and Kilgore 2005; Graunt and Prochazka 2009; Joseph and Butera 2011). Currently, no animal study of myelinated axons has tested frequencies above 50 kHz to observe a monotonic decrease in block threshold. However, animal studies of unmyelinated axons have shown a monotonic decrease in block threshold (Joseph and Butera 2009, 2011). Our recent simulation study using the Hodgkin-Huxley model successfully reproduced the monotonic decrease in block threshold of unmyelinated axon

and revealed a complete deactivation of both sodium and potassium channels as the underlying mechanisms of block (Zhao et al. 2012). Therefore, it is probable that future animal studies of myelinated axons will find a monotonic decrease in block threshold at frequencies above 50 kHz.

Our simulation results also show that the frequency at which the block threshold peaks is higher for a larger diameter axon (Fig.3). This indicates that a higher frequency is required for a larger diameter axon to completely deactivate the sodium and potassium channels. This phenomenon is also observed in our simulation study of unmyelinated axons (Zhao et al. 2012). It might be difficult for animal studies to identify the different peak threshold frequencies in unmyelinated axons due to the small range of the axon diameters (0.5-2 μm) that can only produce a small difference between the different peak threshold frequencies (12-15 kHz). However, it might be possible for animal studies to observe different peak threshold frequencies in myelinated axons because the large range of the axon diameters (2-20 μm) can produce a large difference between the different peak threshold frequencies (80-250 kHz, see Fig.3).

Nerve conduction block induced by high-frequency biphasic electrical stimulation has many potential applications in both clinical medicine and basic neuroscience research (Camilleri et al. 2009; Nashold et al. 1982; Tai et al. 2004; Wattaja et al. 2011). Understanding the mechanisms underlying this type of nerve block could improve the design of new stimulation waveforms (Roth 1994,1995) and further promote clinical application (Leob 1989; Song et al. 2008). Simulation analysis using computer models

provides a tool to reveal the possible blocking mechanisms and may help to design new animal experiments to further improve the nerve blocking method.

APPENDIX

The ionic current $I_{i,n}$ at n^{th} node is described as:

$$I_{i,n} = i_{Na} + i_K + i_P + i_L$$

$$i_{Na} = P_{Na} m^2 h \frac{EF^2}{RT} \frac{[Na]_0 - [Na]_i e^{EF/RT}}{1 - e^{EF/RT}}$$

$$i_K = P_K n^2 \frac{EF^2}{RT} \frac{[K]_0 - [K]_i e^{EF/RT}}{1 - e^{EF/RT}}$$

$$i_P = P_P p^2 \frac{EF^2}{RT} \frac{[Na]_0 - [Na]_i e^{EF/RT}}{1 - e^{EF/RT}}$$

$$i_L = g_L (V_n - V_L)$$

$$E = V_n + V_{rest}$$

where P_{Na} (0.008 cm/s), P_K (0.0012 cm/s) and P_P (0.00054 cm/s) are the ionic permeabilities for sodium, potassium and nonspecific currents respectively; g_L (30.3 $k\Omega^{-1}$ cm^{-2}) is the maximum conductance for leakage current. V_L (0.026 mV) is reduced equilibrium membrane potential for leakage ions, in which the resting membrane potential V_{rest} (-70 mV) has been subtracted. $[Na]_i$ (13.7 mmole/l) and $[Na]_o$ (114.5 mmole/l) are sodium concentrations inside and outside the axon membrane. $[K]_i$ (120 mmole/l) and $[K]_o$ (2.5 mmole/l) are potassium concentrations inside and outside the axon membrane. F (96485 c/mole) is Faraday constant. R (8314.4 mJ/K/mole) is gas constant.

m, h, n and p are dimensionless variables, whose values always change between 0 and 1. m and h represent activation and inactivation of sodium channels, whereas n represents activation of potassium channels. p represents activation of non-specific ion channels. The evolution equations for m, h, n and p are the following:

$$dm/dt = [\alpha_m(1-m) - \beta_m m]k_m$$

$$dh/dt = [\alpha_h(1-h) - \beta_h h]k$$

$$dn/dt = [\alpha_n(1-n) - \beta_n n]k$$

$$dp/dt = [\alpha_p(1-p) - \beta_p p]k$$

and

$$\alpha_m = \frac{0.36(V_n - 22)}{1 - \exp(\frac{22 - V_n}{3})}$$

$$\beta_m = \frac{0.4(13 - V_n)}{1 - \exp(\frac{V_n - 13}{20})}$$

$$\alpha_h = -\frac{0.1(V_n + 10)}{1 - \exp(\frac{V_n + 10}{6})}$$

$$\beta_h = \frac{4.5}{1 + \exp(\frac{45 - V_n}{10})}$$

$$\alpha_n = \frac{0.02(V_n - 35)}{1 - \exp(\frac{35 - V_n}{10})}$$

$$\beta_n = \frac{0.05(10 - V_n)}{1 - \exp(\frac{V_n - 10}{10})}$$

$$\alpha_p = \frac{0.006(V_n - 40)}{1 - \exp(\frac{40 - V_n}{10})}$$

$$\beta_p = -\frac{0.09(V_n + 25)}{1 - \exp(\frac{V_n + 25}{20})}$$

$$k_m = 1.8^{(T-293)/10}$$

$$k = 3^{(T-293)/10}$$

where T is the temperature in °Kelvin. The initial values for m, h, n and p (when $V_n = 0$ mV) are 0.0005, 0.0268, 0.8249 and 0.0049 respectively.

ACKNOWLEDGEMENTS

This study is supported by the NIH under grants DK-068566, DK-090006, DK-091253, and by DOD under grant W81XWH-11-1-0819.

REFERENCES

Ackermann, D.M., Bhadra, N., Gerges, M., Thomas, P.J. (2011). Dynamics and sensitivity analysis of high-frequency conduction block. *Journal of Neural Engineering*, 8, 1-14.

Bhadra, N., & Kilgore, K. (2005). High-frequency electrical conduction block of mammalian peripheral motor nerve. *Muscle Nerve*, 32, 782–790.

Bhadra, N., Lahowetz, E., Foldes, S., Kilgore, K. (2007). Simulation of high-frequency sinusoidal electrical block of mammalian myelinated axons. *Journal of Computational*

Neuroscience, 22, 313-326.

Bowman, B. R., & McNeal, D. R. (1986). Response of single alpha motoneurons to high-frequency pulse train: Firing behavior and conduction block phenomenon. *Applied Neurophysiology*, 49, 121–138.

Boyce, W.E., & Diprima, R.C. (1997). Elementary Differential Equations and Boundary Value Problems. John Wiley & Sons, Inc., 6th ed., pp.436-457.

Camilleri, M., Toouli, J., Herrera, M.F., Kow, L., Pantoja, J.P., Billington, C.J., Tweden, K.S., Wilson, R.R., Moody, F.G. (2009). Selection of electrical algorithms to treat obesity with intermittent vagal block using an implantable medical device. Surgery *for Obesity and Related Diseases*, 5, 224-230.

Frankenhaeuser, B. (1960). Quantitative description of sodium currents in myelinated nerve fibres of xenopus laevis. *Journal of Physiology (Lond.)*, 151, 491-501.

Frankenhaeuser, B., & Huxley, A.F. (1964). The action potential in the myelinated nerve fibre of Xenopus Laevis as computed on the basis of voltage clamp data. *Journal of Physiology (Lond.)*, 171, 302-315.

Gerges, M., Foldes, E.L., Ackermann, D.M., Bhadra, N., Bhadra, N., Kilgore, K.L. (2010). Frequency and amplitude-transitioned waveforms mitigate the onset response in high-frequency nerve block. *Journal of Neural Engineering*, 7, 1-9.

Graunt, R.A., & Prochazka, A. (2009). Transcutaneously coupled, high-frequency electrical stimulation of the pudendal nerve blocks external urethral sphincter contractions. *Neurorehabiliation and Neural Repair*, 23, 615-626.

Hodgkin, A. L., & Huxley, A. F. (1952). A quantitative description of membrane current and its application to conduction and excitation in nerve. *Journal of Physiology (Lond.)*, 117, 500–544.

Joseph, L., & Butera, R. (2009). Unmyelinated aplysia nerves exhibit a nonmonotonic blocking response to high-frequency stimulation. *IEEE Transactions on Neural System and Rehabilitation Engineering*, 17, 537–544.

Joseph, L., & Butera, R. (2011). High-frequency stimulation selectively blocks different types of fibers in frog sciatic nerve. *IEEE Transactions on Neural System and Rehabilitation Engineering*, 19, 550–557.

Leob, G.E. (1989). Neural prosthetic interfaces with the nervous system," *Trends on Neuroscience*, 12, 195-201.

Liu, H., Roppolo, J.R., de Groat, W.C., Tai, C. (2009). The Role of slow potassium current in nerve conduction block induced by high-frequency biphasic electrical current. *IEEE Transactions on Biomedical Engineering*, 56, 137-146.

Nashold, B. S., Goldner, J. L., Mullen, J. B., Bright, D. S. (1982). Long-term pain control by direct peripheral-nerve stimulation. *Journal of Bone Joint Surgery*, 64A, 1–10.

Rattay, F. (1989). Analysis of models for extracellular fiber stimulation," *IEEE Transactions on Biomedical Engineering*, 36, 676-682.

Rattay, F., & Aberham, M. (1993). Modeling axon membranes for functional electrical stimulation. *IEEE Transactions on Biomedical Engineering*, 40, 1201-1209.

Reboul, J., & Rosenblueth, A. (1939). The action of alternating currents upon the

electrical excitability of nerve. *American Journal of Physiology*, 125, 205–215.

Rosenblueth, A., & Reboul, J. (1939) The blocking and deblocking effects of alternating currents on nerve. *American Journal of Physiology*, 125, 251–264.

Roth, B.J. (1994). Mechanisms for electrical stimulation of excitable tissue," *Critical Review on Biomedical Engineering*, 22, 253-305.

Roth, B.J. (1995). A mathematical model of make and break electrical stimulation of cardiac tissue by a unipolar anode or cathode. *IEEE Transactions on Biomedical Engineering*, 42, 1174-1184.

Song, D., Raphael, G., Lan, N., Loeb, G.E. (2008). Computationally efficient models of neuromuscular recruitment and mechanics. *Journal of Neural Engineering*, 5, 175-184.

Tai, C., de Groat, W.C., Roppolo, J.R. (2005a). Simulation analysis of conduction block in unmyelinated axons induced by high-frequency biphasic electrical currents. *IEEE Transactions on Biomedical Engineering*, 52, 1323–1332.

Tai, C., de Groat, W.C., Roppolo, J.R. (2005b). Simulation of nerve block by high-frequency sinusoidal electrical current based on the Hodgkin-Huxley model. *IEEE Transactions on Neural System and Rehabilitation Engineering*, 13, 415-422.

Tai, C., Guo, D., Wang, J., Roppolo, J.R., de Groat, W.C. (2011). Mechanism of conduction block in amphibian myelinated axon induced by biphasic electrical current at ultra-high frequency. *Journal of Computational Neuroscience*, 31, 615-623.

Tai, C., Roppolo, J.R., de Groat, W.C. (2004). Block of external urethral sphincter

contraction by high frequency electrical stimulation of pudendal nerve. Journal of Urology, 172, 2069–2072.

Tai, C., Wang, J., Roppolo, J.R., de Groat, W.C. (2009). Relationship between temperature and stimulation frequency in conduction block of amphibian myelinated axon. *Journal of Computational Neuroscience*, 26, 331-338.

Wattaja, J.J., Tweden, K.S., Honda, C.N. (2011). Effects of high frequency alternating current on axonal conduction through the vagus nerve. *Journal of Neural Engineering*, 8, 056031, 2011.

Zhang, X., Roppolo, J.R., de Groat, W.C., Tai, C. (2006). Mechanism of nerve conduction block induced by high- frequency biphasic electrical currents. *IEEE Transactions on Biomedical Engineering*, 53, 2445–2454.

Zhao, S., Wang, J., Roppolo, J.R., de Groat, W.C., Tai, C. (2012). Mechanisms underlying non-monotonic block of conduction in unmyelinated axons by high-frequency biphasic stimulation. *Journal of Neural Engineering*, submitted.

FIGURE CAPTIONS

Fig.1. Myelinated axonal model used to simulate conduction block induced by high-frequency biphasic electrical current. The inter-node length $\Delta x = 100d$; d is the axon diameter. L is the nodal length. Each node is modeled by a resistance-capacitance circuit based on the FH model. R_a: inter-nodal axoplasmic resistance; R_m: nodal membrane resistance; C_m: nodal membrane capacitance; $V_{a,n}$: intracellular potential at the nth node;

$V_{e,n}$: extracellular potential at the nth node.

Fig.2. Blocking the propagation of action potentials along an myelinated axon by high-frequency biphasic stimulation at different current intensities. High-frequency (120 kHz) stimulation is continuously delivered at the block electrode. An action potential is initiated via the test electrode at 5 ms after starting the high-frequency stimulation, which is propagating towards both ends of the axon. (a). The 120 kHz stimulation blocks the nerve conduction at the intensity of 19.2 mA; (b) Conduction is not blocked by the 120 kHz stimulation at 19.1 mA. The short arrows mark the locations of test and block electrodes along the axon. The white arrow indicates the propagation of an action potential. Axon diameter: 2 μm.

Fig.3. The intensity threshold to block nerve conduction changes with the stimulation frequency. As the frequency increases the block threshold reaches its peak and then gradually decreases. The peak frequency is larger for larger diameter axon.

Fig.4. The changes in membrane potentials, ionic currents and activation/inactivation of ion channels near the block electrode when conduction block occurs as shown in Fig.2 (a). The legends in (d) indicate the distance of each axonal node to the block electrode. Node at 0 mm is under the block electrode. Axon diameter: 2 μm. (a) Change of membrane potentials, (b) Na^+ current, (c) K^+ current, (d) Na^+ channel activation, (e) Na^+ channel inactivation, (f) K^+ channel activation.

Fig.5. The state of ion channel under the block electrode changes with stimulation frequency at the blocking threshold intensity. (a) Na^+ channel activation, (b) Na^+ channel

inactivation, (c) K^+ channel activation. The Na^+ channel is completely closed (m=0) when the frequency is greater than 90 kHz. Axon diameter: 2 μm.

Fig.6. Ion channel activation/inactivation under the block electrode changing with stimulation intensity (a)-(c) at 120 kHz frequency or changing with stimulation frequency (d)-(f) at 19.2 mA intensity. Axon diameter: 2 μm. Block threshold is at 120 kHz and 19.2 mA as indicated by the arrow in (a) and (d). Note: Na^+ channel activation (m) is presented in log scale in (a) and (d).

Fig.7. Changes of membrane potential induced by high-frequency stimulation in a passive axon without sodium and potassium channels. Axon diameter: 2 μ m. (a) change of membrane potential in the passive axon induced by high-frequency stimulation (120 kHz, 19.2mA) after the stimulation was on for 9.5045 ms; (b) No difference between membrane potential under the block electrode induced by high-frequency stimulation (120 kHz, 19.2mA) in axon with passive or active membrane properties. (c) The passive axon membrane under the block electrode is hyperpolarized to about -110 mV [(-40mV)+(-70mV resting potential)] by stimulation of different frequencies (120-250 kHz) at their corresponding block thresholds (8.4-19.2 mA).

Fig.8. Initial action potential induced by high-frequency stimulation at the block threshold intensity changes with stimulation frequency. (a) 90 kHz stimulation at block threshold intensity induces an initial action potential. (b) 120 KHz stimulation at block threshold intensity does not induce an initial action potential. Axon diameter: 2 μm.

Fig.9. The initial transient state of the ion channels under the block electrode induced by

high-frequency stimulation at the blocking threshold intensity. (a) Na^+ channel activation, (b) Na^+ channel inactivation, (c) K^+ channel activation. The Na^+ channel is quickly driven into a completely closed state ($m \approx 0$) when the frequency is greater than 100 kHz. Axon diameter: 2 μm.

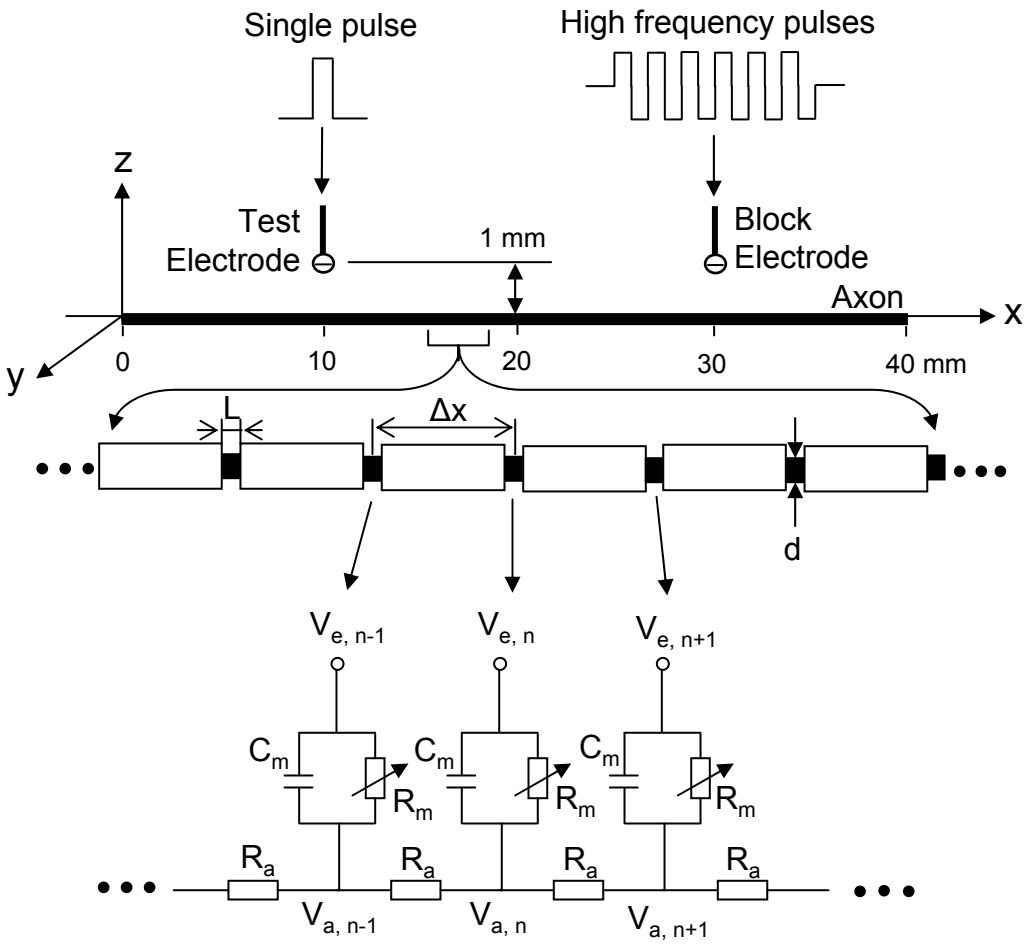

Fig.1. Myelinated axonal model used to simulate conduction block induced by high-frequency biphasic electrical current. The inter-node length $\Delta x = 100d$; d is the axon diameter. L is the nodal length. Each node is modeled by a resistance-capacitance circuit based on the FH model. R_a: inter-nodal axoplasmic resistance; R_m: nodal membrane resistance; C_m: nodal membrane capacitance; $V_{a,n}$: intracellular potential at the n^{th} node; $V_{e,n}$: extracellular potential at the n^{th} node.

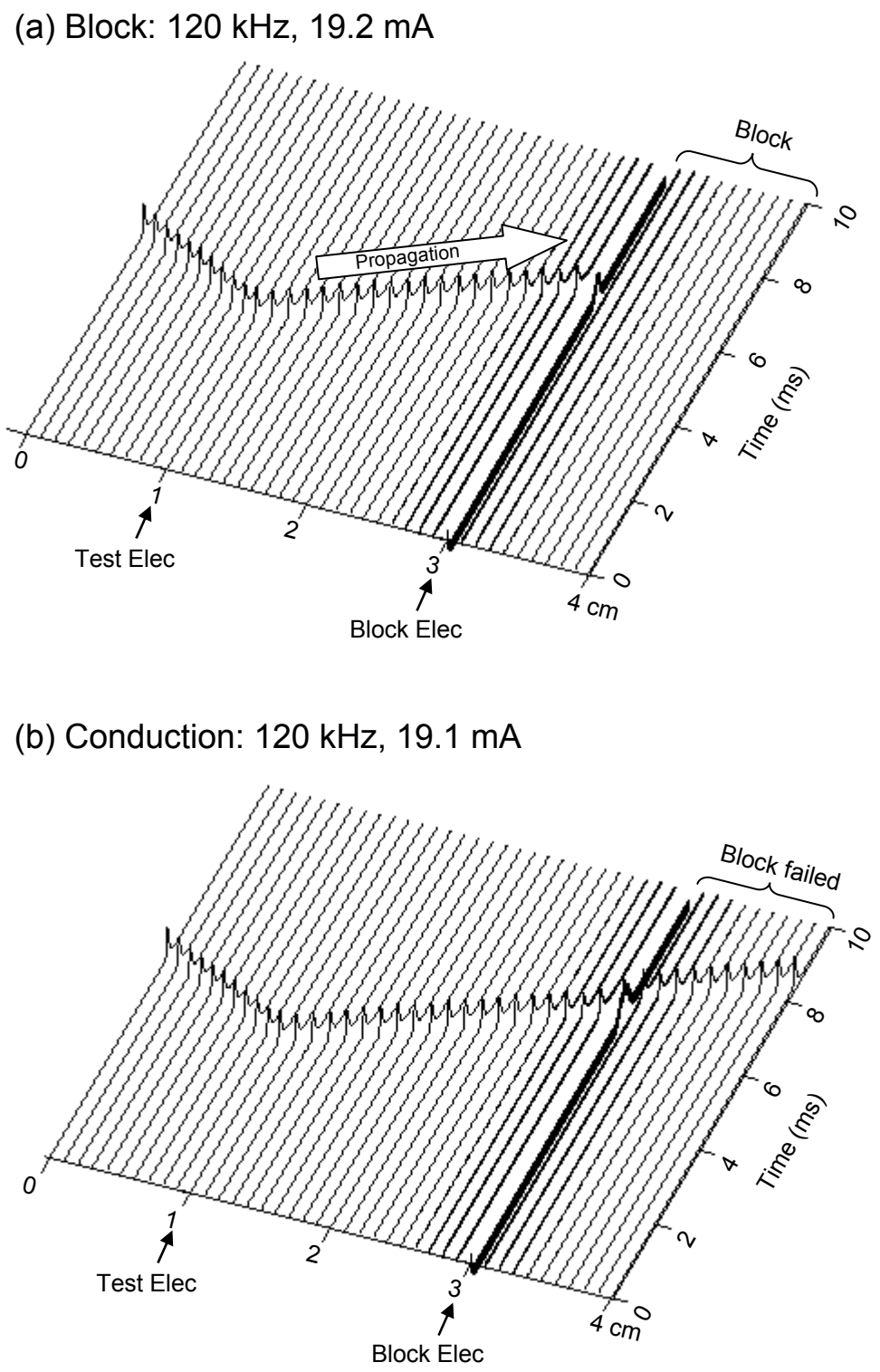

Fig.2. Blocking the propagation of action potentials along an myelinated axon by high-frequency biphasic stimulation at different current intensities. High-frequency (120 kHz) stimulation is continuously delivered at the block electrode. An action potential is initiated via the test electrode at 5 ms after starting the high-frequency stimulation, which is propagating towards both ends of the axon. (a). The 120 kHz stimulation blocks the nerve conduction at the intensity of 19.2 mA; (b) Conduction is not blocked by the 120 kHz stimulation at 19.1 mA. The short arrows mark the locations of test and block electrodes along the axon. The white arrow indicates the propagation of an action potential. Axon diameter: 2 μm.

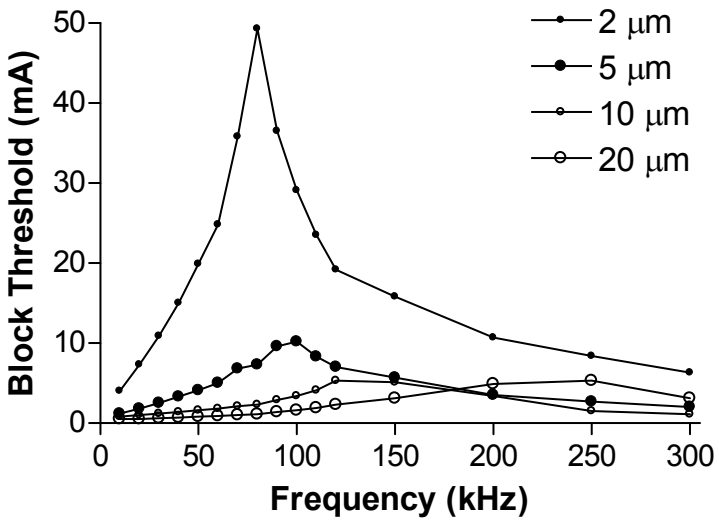

Fig.3. The intensity threshold to block nerve conduction changes with the stimulation frequency. As the frequency increases the block threshold reaches its peak and then gradually decreases. The peak frequency is larger for larger diameter axon.

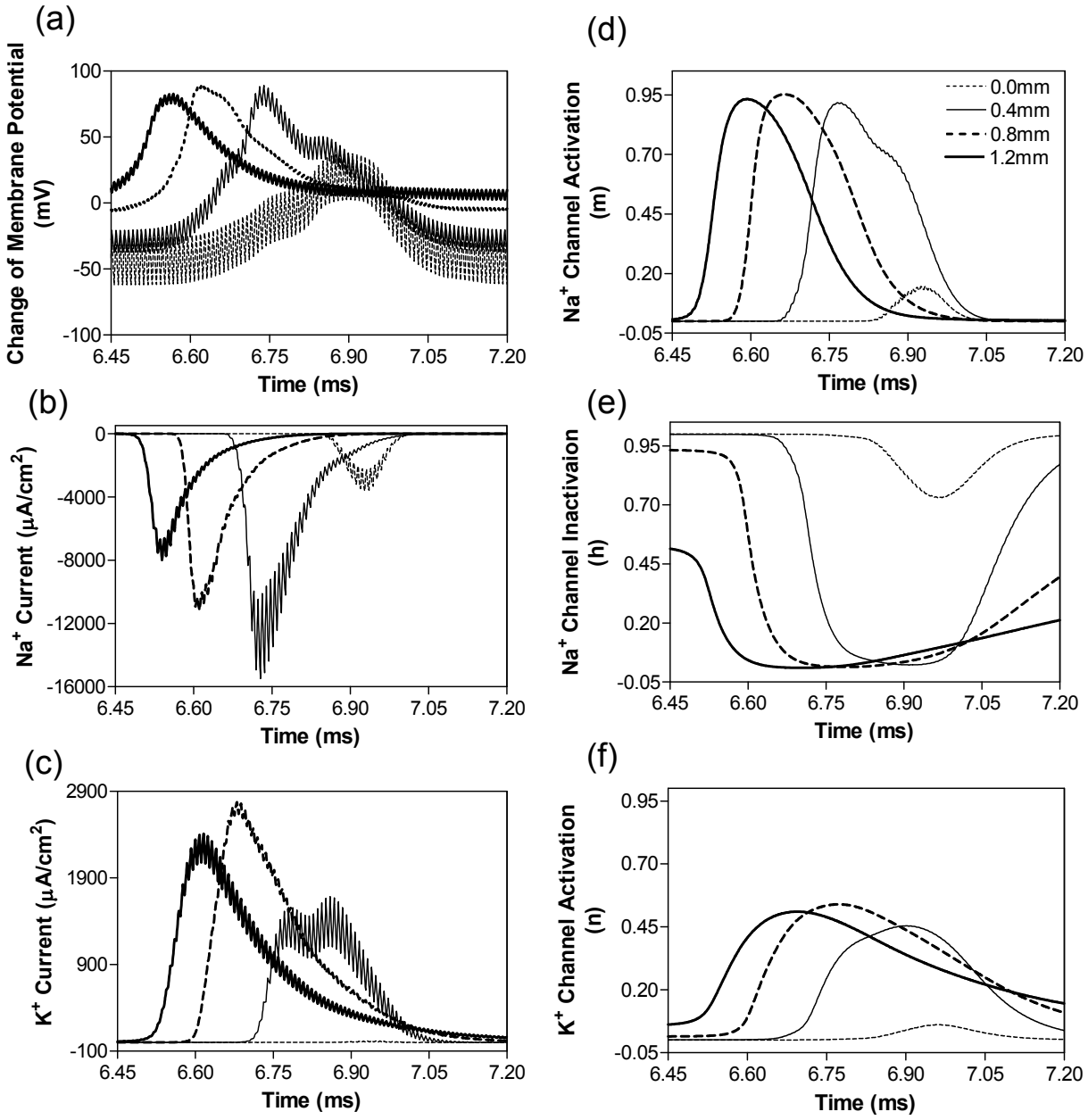

Fig.4. The changes in membrane potentials, ionic currents and activation/inactivation of ion channels near the block electrode when conduction block occurs as shown in Fig.2 (a). The legends in (d) indicate the distance of each axonal node to the block electrode. Node at 0 mm is under the block electrode. Axon diameter: 2 μm. (a) Change of membrane potentials, (b) Na^+ current, (c) K^+ current, (d) Na^+ channel activation, (e) Na^+ channel inactivation, (f) K^+ channel activation.

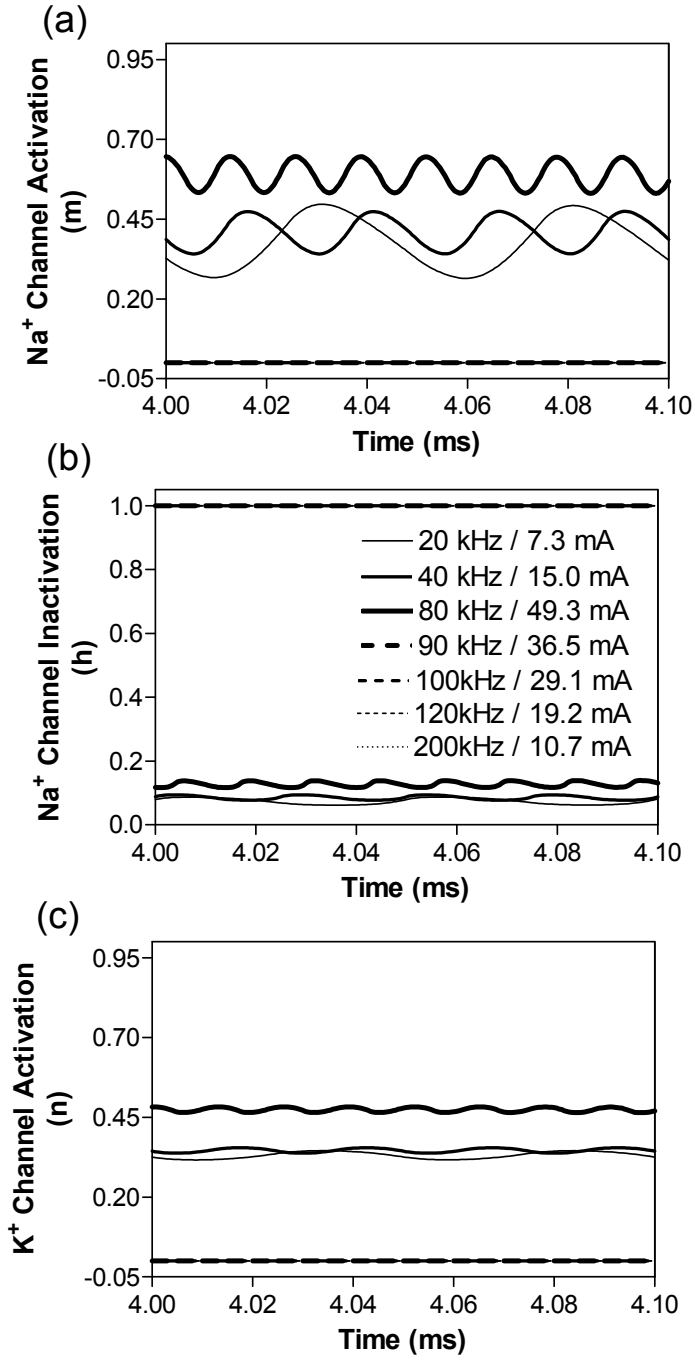

Fig.5. The state of ion channel under the block electrode changes with stimulation frequency at the blocking threshold intensity. (a) Na^+ channel activation, (b) Na^+ channel inactivation, (c) K^+ channel activation. The Na^+ channel is completely closed (m=0) when the frequency is greater than 90 kHz. Axon diameter: 2 μm.

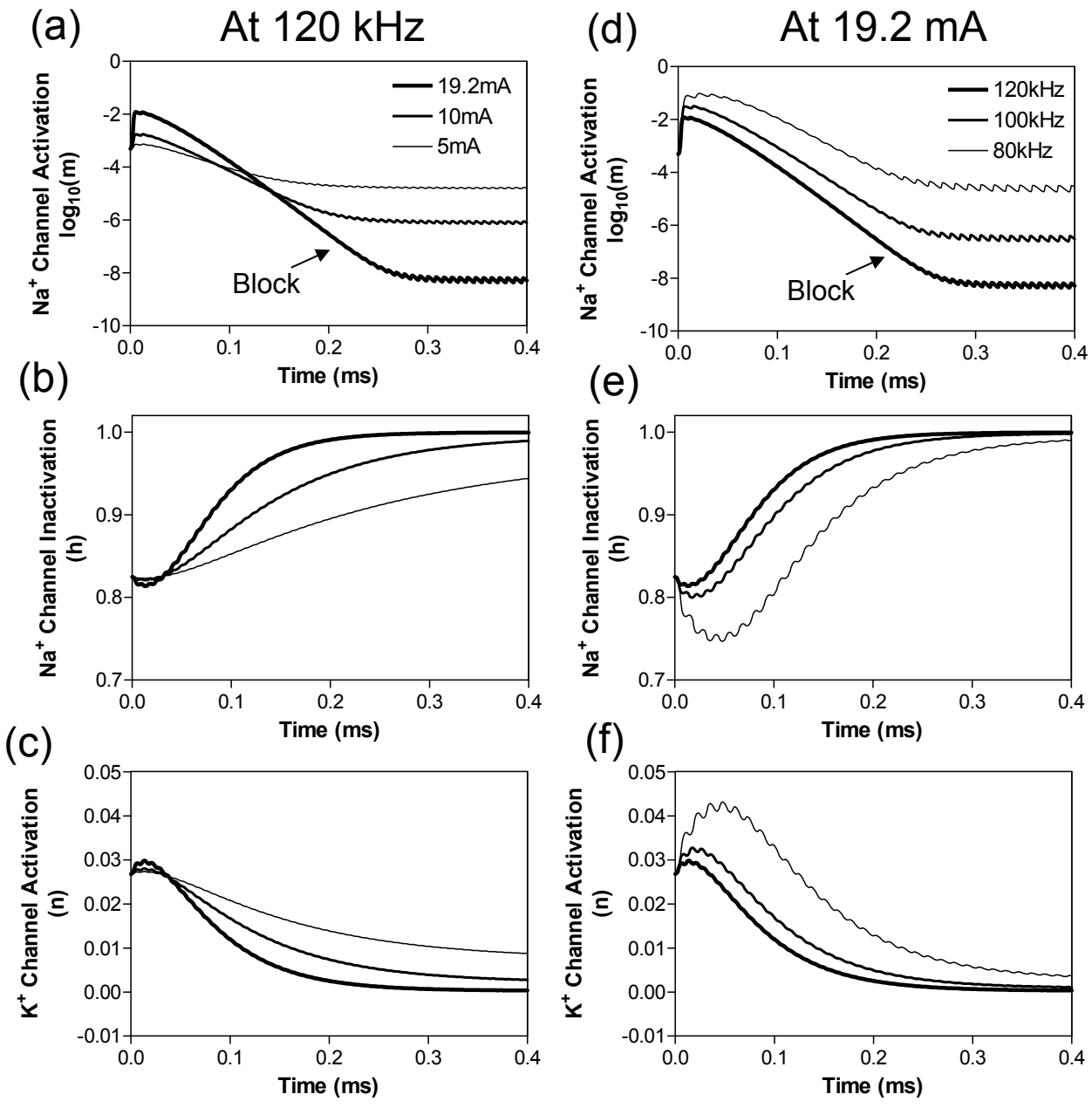

Fig.6. Ion channel activation/inactivation under the block electrode changing with stimulation intensity (a)-(c) at 120 kHz frequency or changing with stimulation frequency (d)-(f) at 19.2 mA intensity. Axon diameter: 2 μm. Block threshold is at 120 kHz and 19.2 mA as indicated by the arrow in (a) and (d). Note: Na^+ channel activation (m) is presented in log scale in (a) and (d).

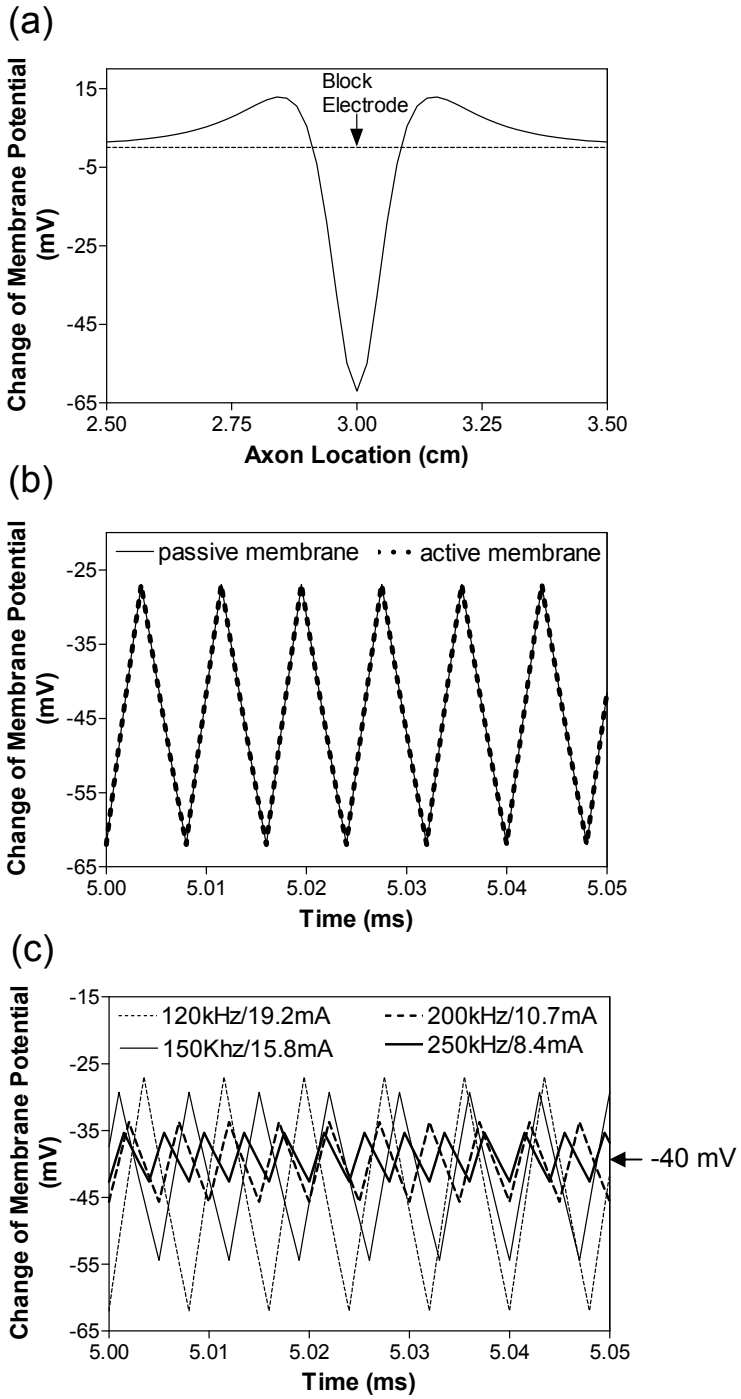

Fig.7. Changes of membrane potential induced by high-frequency stimulation in a passive axon without sodium and potassium channels. Axon diameter: 2 μ m. (a) change of membrane potential in the passive axon induced by high-frequency stimulation (120 kHz, 19.2mA) after the stimulation was on for 9.5045 ms; (b) No difference between membrane potential under the block electrode induced by high-frequency stimulation (120 kHz, 19.2mA) in axon with passive or active membrane properties. (c) The passive axon membrane under the block electrode is hyperpolarized to about -110 mV [(-40mV)+(-70mV resting potential)] by stimulation of different frequencies (120-250 kHz) at their corresponding block thresholds (8.4-19.2 mA).

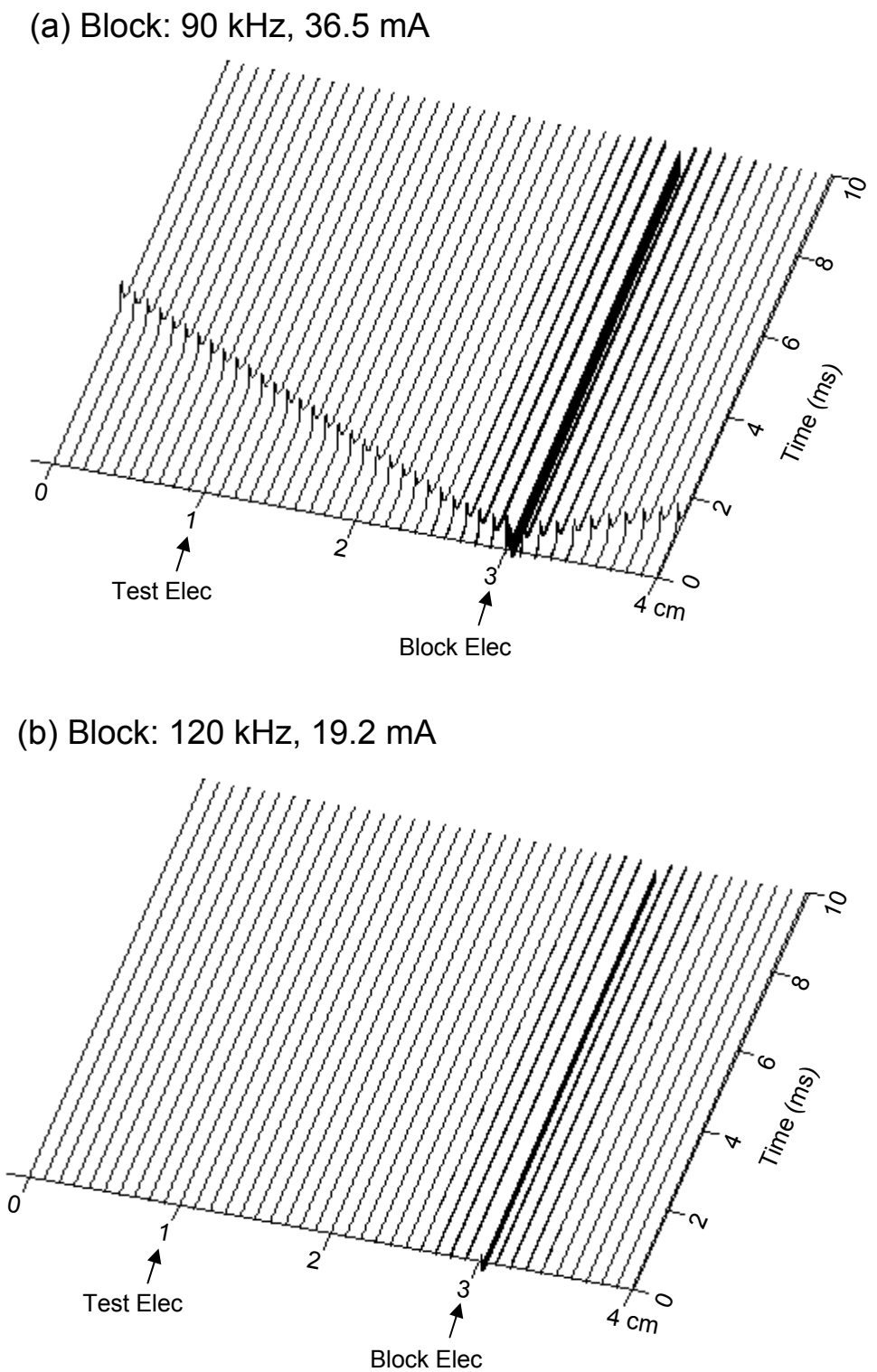

Fig.8. Initial action potential induced by high-frequency stimulation at the block threshold intensity changes with stimulation frequency. (a) 90 kHz stimulation at block threshold intensity induces an initial action potential. (b) 120 KHz stimulation at block threshold intensity does not induce an initial action potential. Axon diameter: 2 μm.

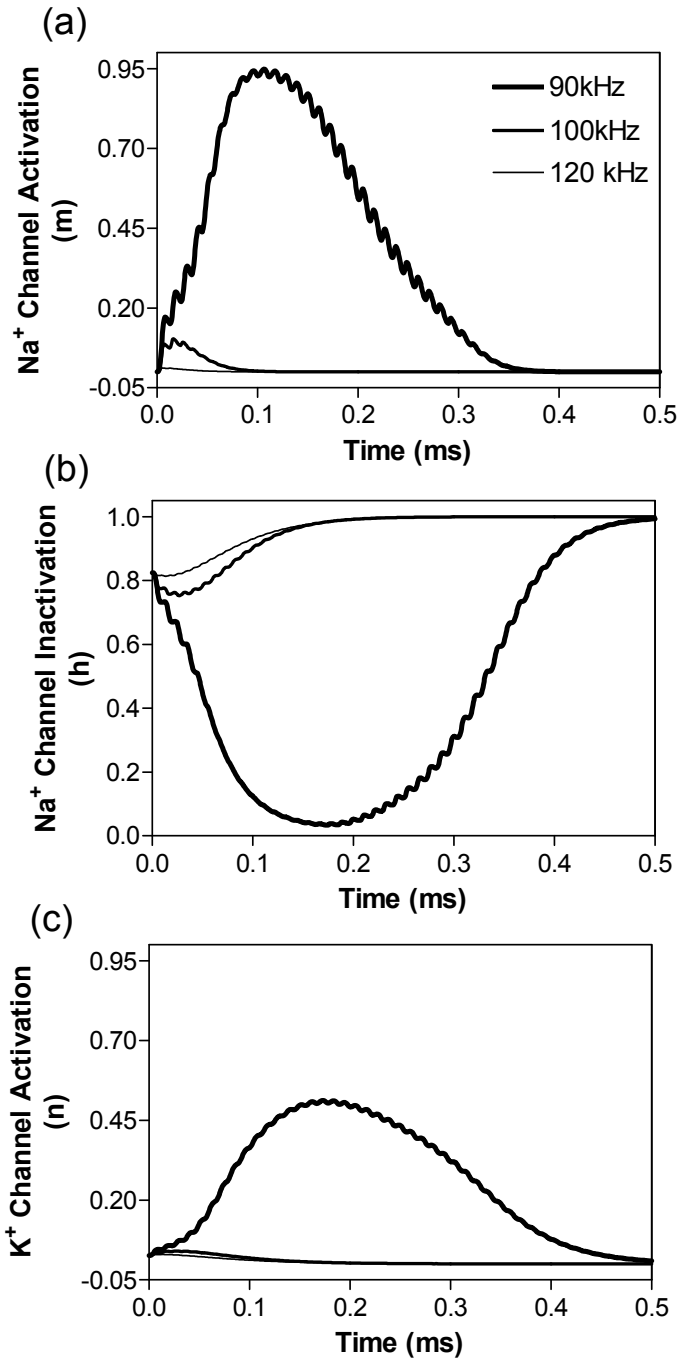

Fig.9. The initial transient state of the ion channels under the block electrode induced by high-frequency stimulation at the blocking threshold intensity. (a) Na^+ channel activation, (b) Na^+ channel inactivation, (c) K^+ channel activation. The Na^+ channel is quickly driven into a completely closed state ($m \approx 0$) when the frequency is greater than 100 kHz. Axon diameter: 2 μm.

AN IMPLANTABLE NEUROPROSTHETIC DEVICE TO RESTORE BLADDER FUNCTION AFTER SCI

Changfeng Tai, PhD
Assistant Professor, University of Pittsburgh

PURPOSE/AIMS: The purpose of this research is to design and develop an implantable neuroprosthetic device to restore urinary bladder function after spinal cord injury (SCI).

DESIGN: We hypothesize that bladder function can be normalized by electrical stimulation and/or blockade of pudendal nerves after chronic SCI using an implantable neuroprosthetic device. Experiments were conducted in cats under both anesthetic and awake conditions to validate our hypothesis. A small (4x5.5x1.4 cm), wireless controlled, wireless chargeable, implantable stimulator was developed for this purpose.

POPULATION/SAMPLE STUDIED: Total 7 cats with chronic SCI were used under α-chloralose anesthesia in this study. One of the cats was also tested under awake condition with the stimulator implanted chronically.

METHODS: Under anesthesia, bladder infusion and pressure measurement was performed via a catheter inserted through the bladder dome. Voiding was induced by slow infusion (0.5-4 ml/min) of the bladder or by electrically stimulating/blocking the pudendal nerves. Under awake condition, bladder empting was performed either by manual expression or by the chronically implanted pudendal nerve stimulator.

DATA ANALYSIS: Voiding efficiency (voided volume/total bladder volume) was compared between bladder distention-induced voiding and pudendal nerve stimulation-induced voiding under anesthesia, and between manual expression and chronically implanted stimulator-induced voiding under awake condition.

FINDINGS: Voiding induced by bladder distention had a very low efficiency (7.3±0.9%) in chronic SCI cats. Electrically stimulating/blocking the pudendal nerves induced efficient (80-90%) voiding under both anesthesia and awake condition.

CONCLUSIONS/RECOMMENDATIONS: Electrically stimulating/blocking the pudendal nerves in cats can successfully restore bladder functions after chronic SCI.

IMPLICATIONS: This animal study indicates that an implantable stimulator might be developed to restore bladder function after chronic SCI in human subjects by electrically stimulating/blocking the pudendal nerves.

FROM/TO TIME PERIOD OF STUDY: September 22, 2011 – October 21, 2014

FUNDING: This study is funded by DOD Spinal Cord Injury Research Program (SCIRP) under contract number W81XWH-11-1-0819.

Mechanisms Underlying Non-monotonic Block of Unmyelinated Axons by High-Frequency Biphasic Stimulation

J. Wang [1], S. Zhao [1,2], J. R. Roppolo [3], W. C. de Groat [3], C. Tai [1]

[1] Department of Urology, University of Pittsburgh, Pittsburgh, PA
[2] Department of Biomedical Engineering, Beijing Jiaotong University, P.R. China
[3] Department of Pharmacology and Chemical Biology, University of Pittsburgh, PA

Axonal conduction block induced by high-frequency biphasic electrical current is investigated using a lumped circuit model of the unmyelinated axon based on Hodgkin-Huxley equations. Axons of different diameters (1 and 2 μm) can be blocked completely when the stimulation frequency is between 5 kHz and 100 kHz. The non-monotonic relationship between block threshold and stimulation frequency, recently discovered in unmyelinated axons of sea-slugs and frogs, is successfully reproduced. Our simulation reveals that complete deactivation of sodium channels by the high-frequency blocking stimulation is the mechanism underlying the decrease in block threshold as the frequency increases above 20 kHz. At a relatively higher frequency (>30 kHz), the high-frequency blocking stimulation can quickly deactivate the sodium channels at the beginning of the stimulation, thereby avoiding the generation of initial action potentials. This simulation study further increases our understanding of conduction block in unmyelinated axons induced by high-frequency biphasic electrical current, and can guide future animal experiments as well as optimize stimulation parameters that might be used for electrically induced nerve block in clinical applications.

Key words: nerve, block, simulation, high-frequency, model.

Supported by: DOD Spinal Cord Injury Research Program (SCIRP) under contract number W81XWH-11-1-0819.